SUPPORTING INFORMATION

Carborane-stilbene dyads: influence of the substituents and cluster isomers on the photoluminescence properties†

A. Ferrer-Ugalde,[a#] J. Cabrera-González,[a] E. J. Juárez-Pérez,[a#] F. Teixidor,[a] E. Pérez-Inestrosa,[b,c] J. M. Montenegro,[b,c] R. Sillanpää,[d] M. Haukka and [d] R. Núñez*[a]

[a] *Institut de Ciència de Materials de Barcelona (ICMAB-CSIC), Campus U.A.B., 08193, Bellaterra, Barcelona, Spain. E-mail: rosario@icmab.es*

[b] *Universidad de Málaga, IBIMA, Department of Organic Chemistry, 29071-Malaga, Spain.*

[c] *Andalusian Centre for Nanomedicine and Biotechnology-BIONAND, Parque Tecnológico de Andalucía, 29590-Málaga, Spain.*

[d] *Department of Chemistry, University of Jyväskylä, FIN-40014, Jyväskylä, Finland.*

† A. Ferrer-Ugalde current address: School of Chemistry and Chemical Engineering. Queen's University of Belfast, David Keir Building, Belfast, BT9 5AG, United Kingdom; E. J. Juárez-Pérez current address: Energy Materials and Surface Sciences Unit (EMSS), Okinawa Institute of Science and Technology Graduate University (OIST), 1919-1 Tancha, Onna-son, Okinawa, 904-0495, Japan

Figure Captions and Tables

Experimantal Part

Instrumentation.

Elemental analyses were performed using a Carlo Erba EA1108 microanalyzer. IR spectra were recorded from KBr pellets on a Shimadzu FTIR-8300 spectrophotometer. The ^{1}H NMR (300.13 MHz), $^{11}B\{^{1}H\}$ and ^{11}B NMR (96.29 MHz) and $^{13}C\{^{1}H\}$ NMR (75.47 MHz) spectra were recorded on a Bruker ARX 300 spectrometer. All NMR spectra were recorded in $CDCl_3$ or CD_3COCD_3 solutions at 25ºC. Chemical shift values for $^{11}B\{^{1}H\}$ NMR spectra were referenced to external $BF_3{\cdot}OEt_2$, and those for ^{1}H and $^{13}C\{^{1}H\}$ NMR were referenced to $SiMe_4$. Chemical shifts are reported in units of parts per million downfield from reference, and all coupling constants are reported in Hertz. MALDI-TOF-MS mass spectra were recorded in the negative ion mode using a Bruker Biflex MALDI-TOF [N2 laser; λexc 337 nm (0.5 ns pulses); voltage ion source 20.00 kV (Uis1) and 17.50 kV (Uis2)]. UV-Vis spectra were recorded on Shimadzu UV-1700 Pharmaspec spectrophotometer, in 0.1 cm cuvettes, using solutions of compounds with 10^{-6} $mol{\cdot}L^{-1}$ of concentration. The fluorescence emission spectra were recorded in a JASCO FP-750 spectrofluorometer and a FLS 920 from Edinburgh Instruments using a 450W Xe lamp as excitation source. Samples were prepared in spectroscopic grade solvents and adjusted to a response within the linear range. No fluorescent contaminants were detected on excitation in the wavelength region of experimental interest. Fluorescence quantum yields were determined by comparison with styrene or stilbene as reference, and corrected for the refractive index of the solvent, cyclohexane for styrene (n = 1.426) and methylcyclohexane for stilbene (n = 1.422). Samples were prepared in such a way as to obtain an absorbance of 0.1–0.2 at the excitation wavelength to avoid internal reabsorption effects in the posterior emission.[1] The quantum yield for *i* was determined by $\Phi_i = [(F_i{\cdot}A_R{\cdot}n_i^2)/ (F_R{\cdot}A_i{\cdot}n_R^2)]{\cdot}\Phi_{R,}$ where f_i = 1-

10^{-Ai}, F are the integrated intensities, A the absorbances and n the refractive indices.[2] The aggregates of **10** and **14** were obtained by adding water to THF solutions of both compounds and stirring.[3-5] The solid state (powder and films) fluorescence emission measurements were carried out in an Edinburgh Instrument FLS920 fluorometer, using a 450 W Xe lamp as excitation source and a Starna 20-C support for solid samples. The excitation wavelength used was 310 nm and the spectra were registered using 2 nm excitation and emission slits opening and a dwell time of 0.2 s. For the preparation of films a drop of a solution of **10** and **14** was evaporated over a short path length demountable Starna 20C cell and then the emission spectra were registered.

X-ray Structure Determinations.

The crystals of **6**, **7**, **9**, **12**, **13**, **14**, and **15** were immersed in cryo-oil, mounted in MiTeGen loops, and measured at 120-123 K. The X-ray diffraction data were collected on a Rigaku Oxford Diffraction Supernova diffractometer using Cu Kα (λ = 1.54184 Å) radiation or on a Nonius Kappa ApexII diffractometer using Mo Kα (λ = 0.71073 Å) radiation. The Denzo/Scalepack[6] or CrysAlisPro[7] program packages were used for cell refinements and data reductions. The structures were solved by direct methods or by charge flipping method using the SHELXS-97[8] or Superflip[9] programs. A multi-scan or Gaussian absorption correction (SADABS[10] or CrysAlisPro[7]) was applied to structural data of **6**, **7**, **12**, **14**, and **15**. Structural refinements were carried out using SHELXL-97 or SHELXL-2014[8] programs. The unit cell of structures **9** and **12** contained two independent molecules. In structure **9**, carbon atoms in the double bond between the aromatic rings in one of the stilbene ligands were disordered over two sites. Structure **12** was refined as a racemic twin. The BASF value was refined to 0.017. In all structures the hydrogen atoms were positioned geometrically and constrained to ride on their

parent atoms with C-H = 0.95-0.99 Å, B-H 1.12 Å, and U_{iso} = 1.2-1.5·U_{eq} (parent atom). Crystallographic details are summarized in Table 2 and Table S2. Selected bond lengths are given in Table S1. The codes for structures **6-15** are CCDC 1507869-1507875

Calculations.

Ground-state calculations were carried out by using hybrid DFT (B3LYP functional) and Ahlrichs def2-TZV basis set[11, 12] as implemented in the ORCA 3.0.1 package.[13] Partial density of state (PDOS) of the fragments fluorophore (styrenyl or stilbenyl), carboranyl substituent (Me or Ph) and carborane cage (*o*-, *m*- or *p*-carborane) and their orbital composition analysis (Mulliken type with 0.5 eV of FWHM) were obtained using Multiwfn 3.3.7.[14, 15] Probabilty (60 %) isodensity for the HOMO – LUMO 3D contour plots of the compounds were obtained using Gabedit.[16]

Characterization of compounds 3-16

The IR spectra show typical υ(B-H) strong bands for *closo* clusters between 2565 and 2592 cm^{-1}. The ^{1}H NMR spectra of **3-16** show one singlet in a region from δ 3.06 to 3.49 ppm due to the C_c-CH_2 protons, which is slightly upfield shifted (0.1-0.2 ppm) in the *m*-derivatives with regard to *o*-isomers. For compounds **3-4** the vinyl protons appear in the region 5.28-6.74 ppm as a set of three resonances, similar to their analogous *o*-carborane derivatives **1-2**.[17] These signals disappear completely after the Heck reaction, corroborating the formation of compounds **9-16**, in which a resonance attributed to the two alkene protons is observed in the range 7.03-7.14 ppm. The ^{13}C NMR spectra of **3-16** show one resonance in the range 40.34-42.95 ppm attributed to the C_c-CH_2 carbons, whereas compounds **5-8** show one signal at around 93 ppm attributed to *C*-I. All the

stilbene-containing carboranes **9-16** show resonances in the aromatic region from δ 120 to 140 ppm.

The $^{11}B\{^{1}H\}$ NMR resonances of *o*-carborane derivatives appear in the typical *closo* region,[18] from δ -3.59 to -10.55 ppm, with the general pattern 2:8 for Ph-*o*-carborane derivatives and 1:1:4:4 or 1:1:8 for Me-*o*-carborane derivatives. Additionally, resonances for *m*-carborane derivatives appear in the region from δ -5.09 to -13.73 ppm with patterns 1:1:6:2 or 2.6:2. Elemental analyses and MALDI-TOF spectrometry also confirmed the structures of all these compounds (see Experimental Part).

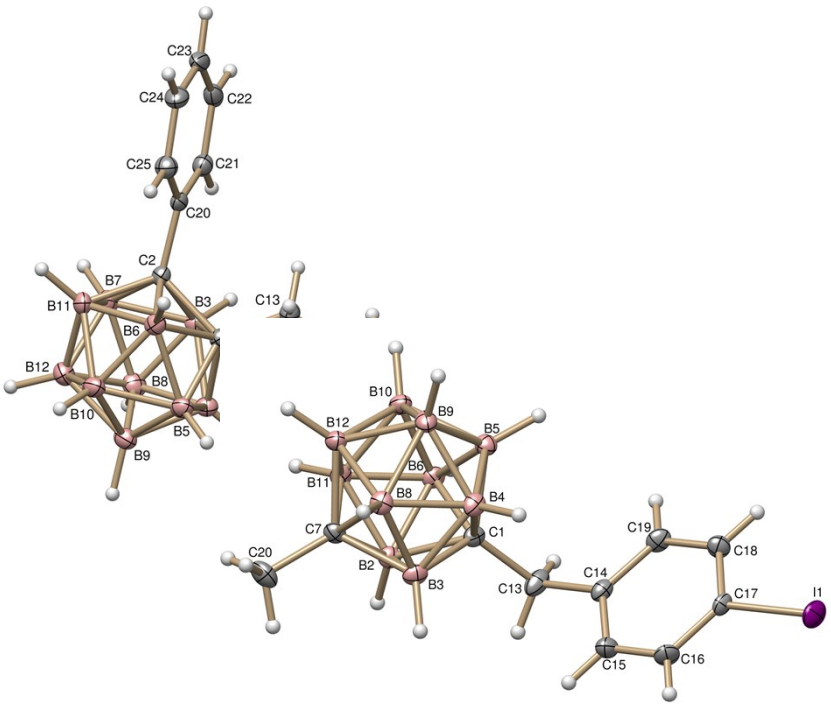

Fig. S1 Ortep plot of the solid-state structure of **6**.

Fig. S2 Ortep plot of the solid-state structure of **7**.

Compound **6** crystallized in the orthorhombic space group Pbca, whereas compound **7** crystallized in the monoclinic space group $P2_1/n$. Both compounds show weak intramolecular interactions. The iodine substituent (I1) of the iodobenzyl group is involved in a very weak hydrogen bond with the adjacent B7-H7 unit (B7···I1$^{\#1}$: 3.977(3) Å, #1: -½-x, -y, -½+z) in **6**, and with the adjacent B(10)-H(10) (B10···I1$^{\#2}$: 3.853(3) Å, #2: ½-x, ½-y, ½-z) in **7** (Table S3). Structure of **9** consists of two independent molecules. The organic moieties are connected through series of very weak C-H···π contacts between the stilbene ligands in **9** (Fig. S3) and in **12** (Fig. S4) where the stilbene group is acting as a terminal substituent. Unlike **9**, in **12** the carborane ends of the molecules are pushed further apart by the CH_3 groups. In compound **13** the stilbene ligands are forming parallel stacks with very weak π···π interactions (Fig. S5). The chains are pulled together via interactions between the carborane units giving an overall zig-zag structure. In **14** the phenyl substituents on carbon C2 force the carborane

ends of the molecules apart; reducing the direct contacts between carborane cages (Fig. S6). In compound **15** the stilbene ligands are well separated and not involved even in weak in π-interactions (Fig. S7).

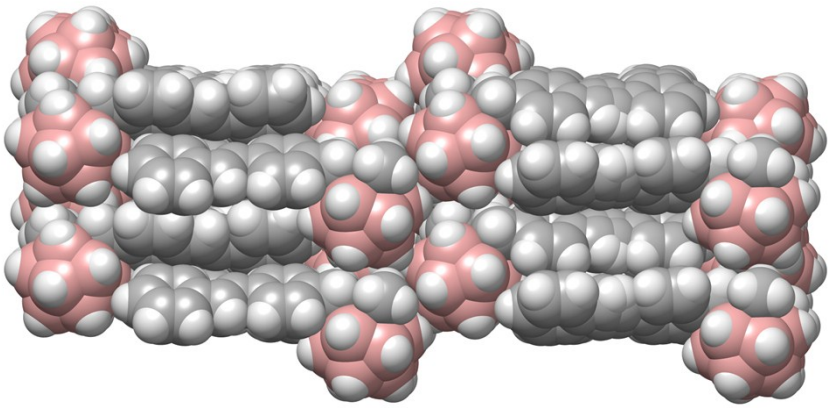

Fig. S3 Packing of **9** along crystallographic c-axis.

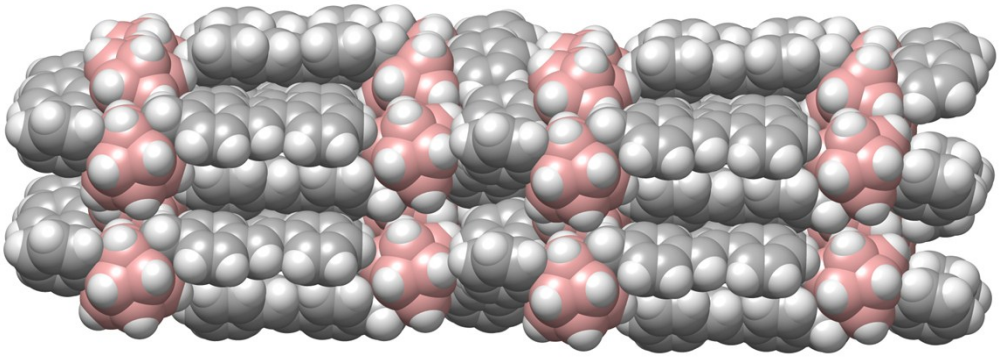

Fig. S4 Packing of **12** along crystallographic a-axis.

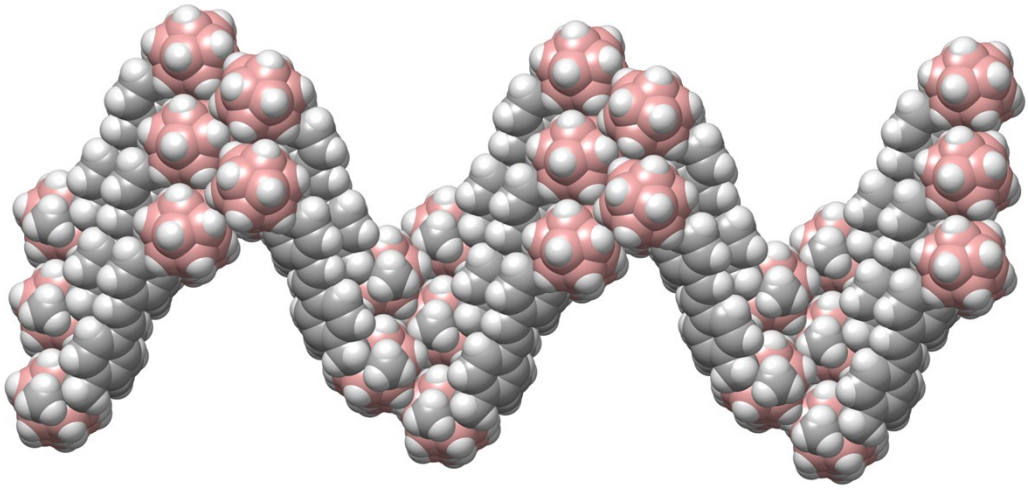

Fig. S5 Packing of **13** along crystallographic c-axis.

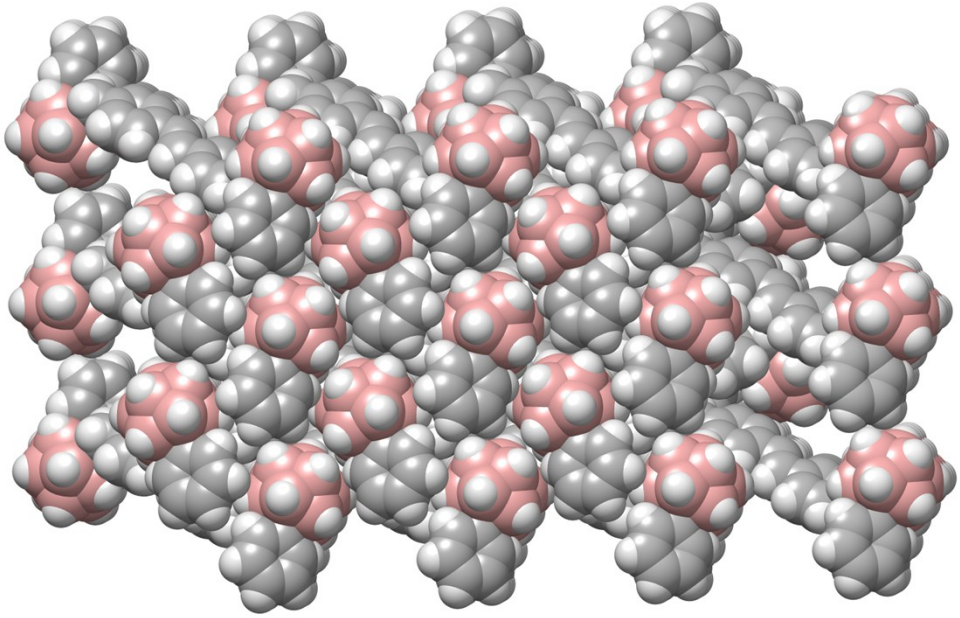

Fig. S6 Packing of **14** along crystallographic a-axis.

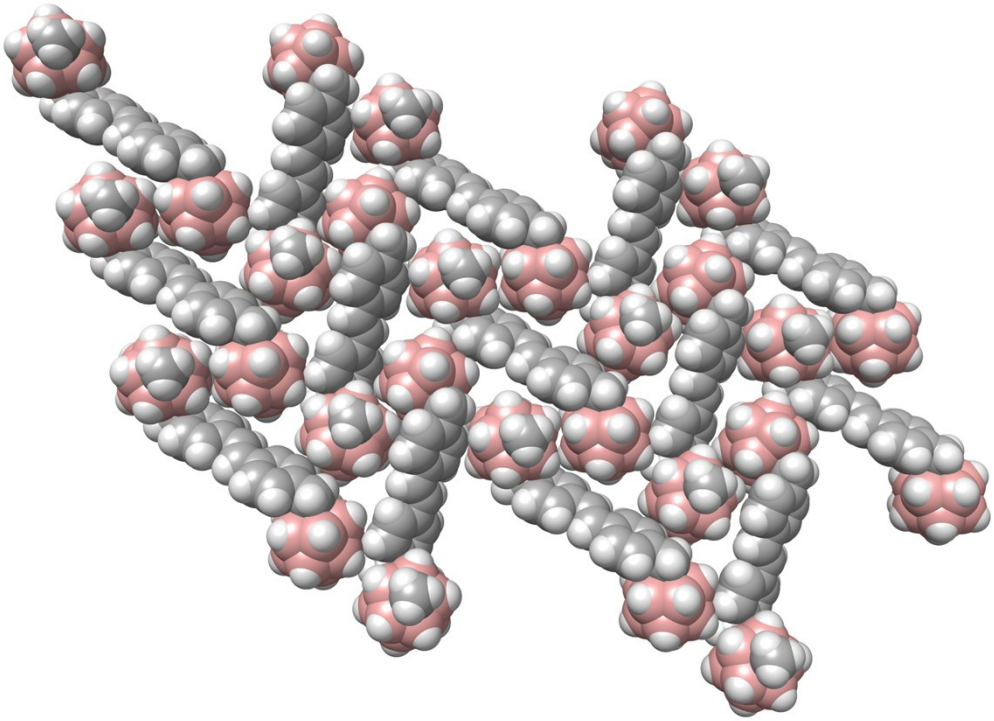

Fig. S7 Packing of **15** on crystallographic ab-plane.

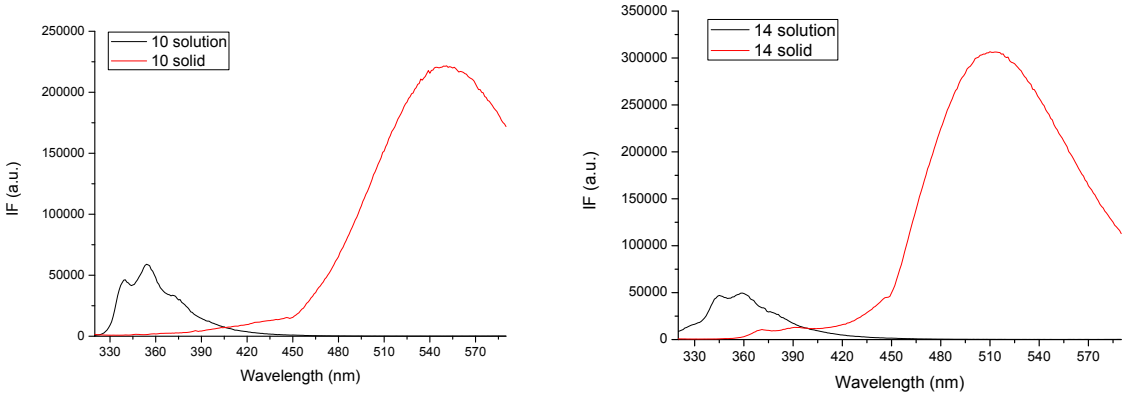

Fig. S8 Emission spectra of **10** and **14** in solution (THF) and solid at λ_{exc} = 310 nm.

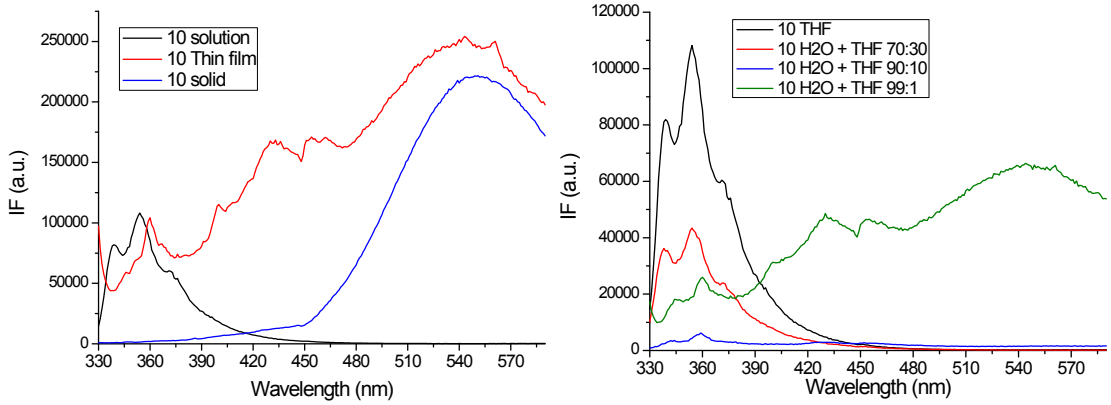

Fig. S9 Emission spectra of **10** in solution (THF), solid and thin film at λ_{exc} = 310 nm (left). Fluorescence emission of **10** in different THF/H_2O ratios at λ_{exc} = 320 nm (right).

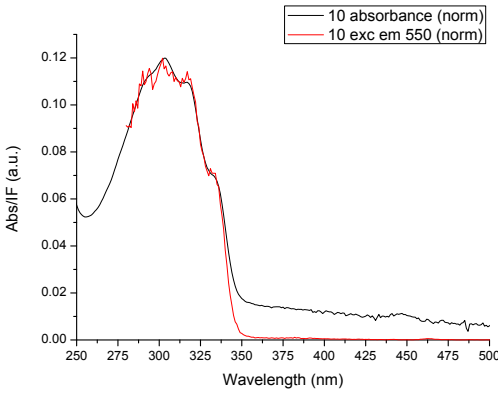
10 absorbance (norm)
10 exc em 550 (norm)
Abs/IF (a.u.)
Wavelength (nm)

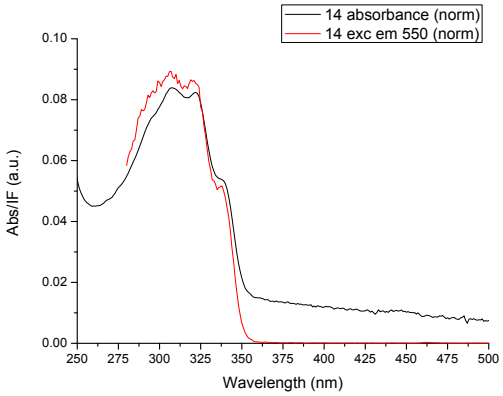
14 absorbance (norm)
14 exc em 550 (norm)
Abs/IF (a.u.)
Wavelength (nm)

Fig S10. Absorbance and excitation spectra of **10** and **14** in THF and H_2O/THF 97:3, respectively.

Table S1. Selected bond lenghts (Å).

	6	**7**	**9A**	**9B**	**12A**	**12B**	**13**	**14**	**15**
C(1)-C(13)	1.527(3)	1.536(3)	1.531(2)	1.535(2)	1.537(9)	1.543(8)	1.531(2)	1.527(2)	1.5407(14)
C(2)-C(20)	1.504(3)								
C(17)-I(1)	2.105(2)								
C(1)-I(1)		2.100(2)							
C(7)-C(20)		1.521(3)							
C(7)-C(21)									1.5216(15)
C(2)-C(28)			1.514(2)	1.510(2)					
C(20)-C(21)			1.332(2)		1.339(9)	1.348(8)			
C(7)-C(28)					1.506(8)	1.498(8)			
C(2)-C(21)							1.513(2)	1.503(2)	
C(20)-C(20)[#]							1.335(3)[#1]	1.313(4)[#2]	1.325(2)[#3]

Symmetry transformations used to generate equivalent atoms: #1: -x+2,-y,-z+2, #2: -x,-y,-z, #3: -x,-y+2,-z

Table S2. Selected crystallographic data for compounds **6**, **7**, **9** and **12-15**.

	6	**7**	**9**	**12**	**13**	**14**	**15**
empirical formula	$C_{15}H_{21}B_{10}I$	$C_{10}H_{19}B_{10}I$	$C_{18}H_{26}B_{10}$	$C_{23}H_{28}B_{10}$	$C_{22}H_{40}B_{20}$	$C_{32}H_{44}B_{20}$	$C_{22}H_{40}B_{20}$
fw	436.32	374.25	350.49	412.55	520.74	644.87	520.74
temp (K)	123(2)	123(2)	123(2)	120(2)	123(2)	123(2) K	123(2)
λ(Å)	0.71073	1.54184	0.71073	1.54178	0.71073	1.54184 Å	1.54184
cryst syst	Orthorhombic	Monoclinic	Monoclinic	Monoclinic	Monoclinic	Monoclinic	Monoclinic
space group	Pbca	$P2_1/n$	$P2_1/n$	$P2_1$	$P2_1/n$	$P2_1/c$	$P2_1/c$
a (Å)	8.0897(2)	7.75300(10)	11.9556(3)	11.4530(10)	6.6255(2)	14.4906(3)	12.0182(2)
b (Å)	21.1818(5)	17.9867(3)	7.5223(2)	7.2953(6)	28.5036(10)	12.2981(2)	12.79780(10)
c (Å)	22.1298(4)	11.8559(2)	45.0299(9)	27.575(2)	8.0673(3)	10.38440(10)	10.95890(10)
β (deg)	90	98.493(2)	92.6080(10)	97.317(8)	95.529(2)	91.1570(10)	113.436(2)
V (Å^3)	3792.04(15)	1635.19(4)	4045.51(17)	2285.2(3)	1516.43(9)	1850.19(5)	1546.50(4)
Z	8	4	8	4	2	2	2
ρ_{calc} (Mg/m^3)	1.529	1.520	1.151	1.199	1.14	1.158	1.118
μ(Mo Kα) (mm^{-1})	1.684	15.173	0.057	0.438	0.054	0.404	0.367
No. reflns.	22686	21644	41836	14078	5247	25257	38438
Unique reflns.	3704	3447	7837	7331	2968	3902	3255
GOOF (F^2)	1.046	1.044	1.015	1.050	1.049	1.064	1.057
R_{int}	0.0281	0.0423	0.0399	0.0915	0.0216	0.0599	0.0357
R1[a] ($I \geq 2\sigma$)	0.0226	0.0287	0.0541	0.0980	0.0487	0.0627	0.0430
wR2[b] ($I \geq 2\sigma$)	0.0491	0.0769	0.1345	0.2676	0.1277	0.1735	0.1213

[a] $R1 = \Sigma||F_o| - |F_c||/\Sigma|F_o|$. [b] $wR2 = [\Sigma[w(F_o^2 - F_c^2)^2]/ \Sigma[w(F_o^2)^2]]^{1/2}$.

Table S3. Weak hydrogen bonds in **6** and **7**.

Compound	Bond	D-H	H···A	D···A	D-H···A
6	B7···I1[1]	1.12	3.316	3.977(3)	118.7
7	B10···I1[2]	1.12	3.207	3.853(3)	117.4

#1: -½-x, -y, -½+z, #2: ½-x, ½-y, ½-z

Table S4. Molecular orbital contribution (%) for the fragments constituting every compound.

				MO % contribution		
Compounds	**Carborane**	**Orbital type**	**Energy (eV)**	**Ph/Me**	**Styrenyl/stilbenyl**	***o-/m-/p*-carboranyl**
1	*o*-Me	LUMO	-1.48	0.10	96.70	3.20
		HOMO	-6.47	0.10	98.20	1.70
2	*o*-Ph	LUMO	-1.52	58.90	18.87	22.20
		HOMO	-6.42	0.30	98.03	1.72
3	*m*-Me	LUMO	-1.31	0.10	97.03	2.94
		HOMO	-6.32	0.02	98.27	1.71
4	*m*-Ph	LUMO	-1.34	1.39	94.84	3.77
		HOMO	-6.32	0.30	98.13	1.63
	p-Me	LUMO	-1.32	0.20	96.35	3.54
		HOMO	-6.29	0.02	98.17	1.80
	p-Ph	LUMO	-1.32	0.89	95.00	4.11
		HOMO	-6.30	0.10	98.14	1.74
9	*o*-Me	LUMO	-1.90	0.10	98.10	1.80
		HOMO	-5.94	0.02	99.20	0.78
10	*o*-Ph	LUMO	-1.82	2.85	94.84	2.31
		HOMO	-5.85	0.14	99.06	0.80
11	*m*-Me	LUMO	-1.78	0.00	98.15	1.84
		HOMO	-5.85	0.01	99.31	0.68
12	*m*-Ph	LUMO	-1.80	0.04	98.06	1.90
		HOMO	-5.83	0.00	99.15	0.85

13	2 *x o*-Me	LUMO	-2.02	0.11	97.74	2.15
		HOMO	-6.01	0.06	98.27	1.67
14	2 *x o*-Ph	LUMO	-2.00	1.22	95.42	3.36
		HOMO	-5.97	0.17	98.07	1.76
15	2 *x m*-Me	LUMO	-1.97	0.02	97.58	2.40
		HOMO	-5.95	0.01	98.07	1.92
16	2 *x m*-Ph	LUMO	-1.92	0.07	96.83	3.10
		HOMO	-5.91	0.02	98.38	1.60

NMR Spectra

Compound **3**

^{1}H NMR ($CDCl_3$, TMS)

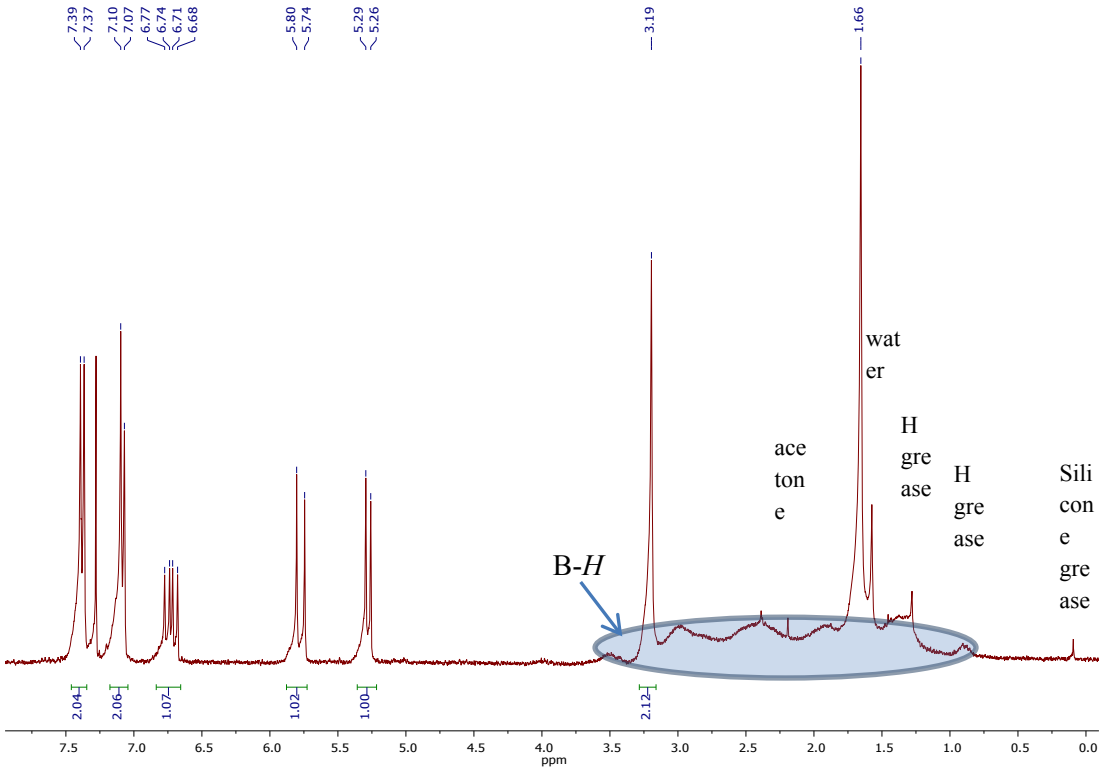

$^{1}H\{^{11}B\}$ NMR ($CDCl_3$, TMS)

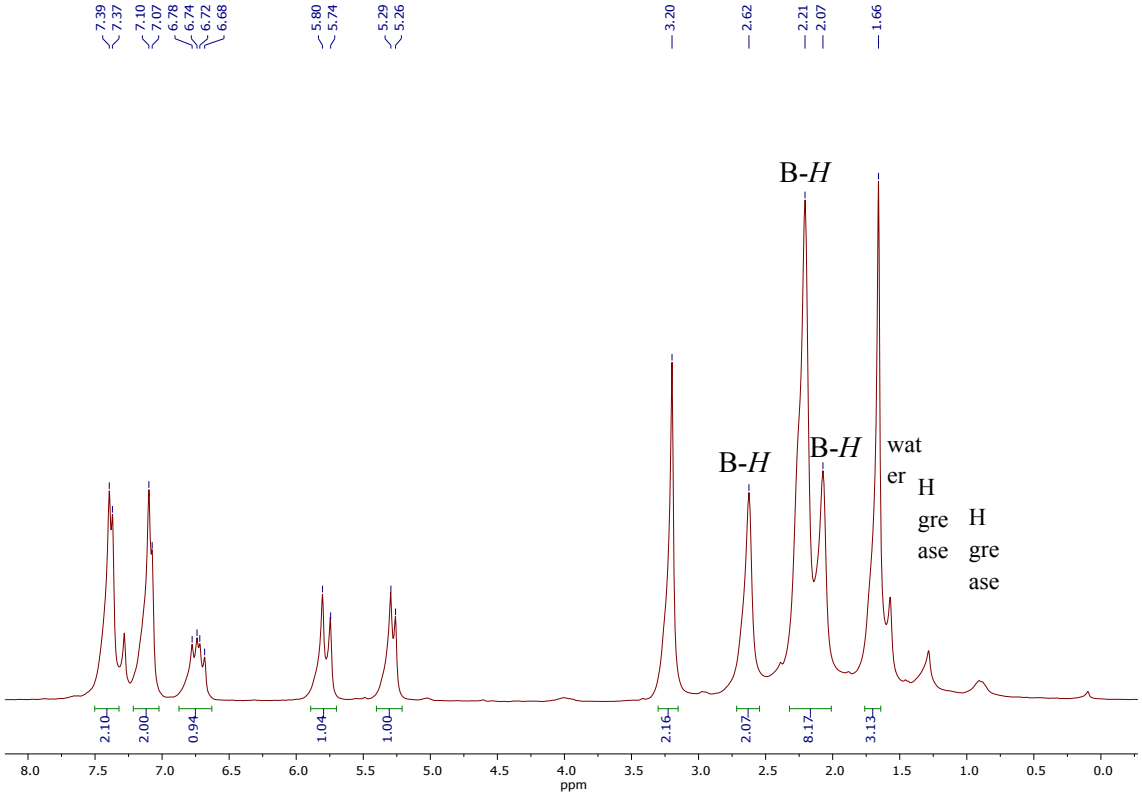

$^{11}B\{^{1}H\}$ NMR (CD_3COCD_3, $BF_3 \cdot Et_2O$)

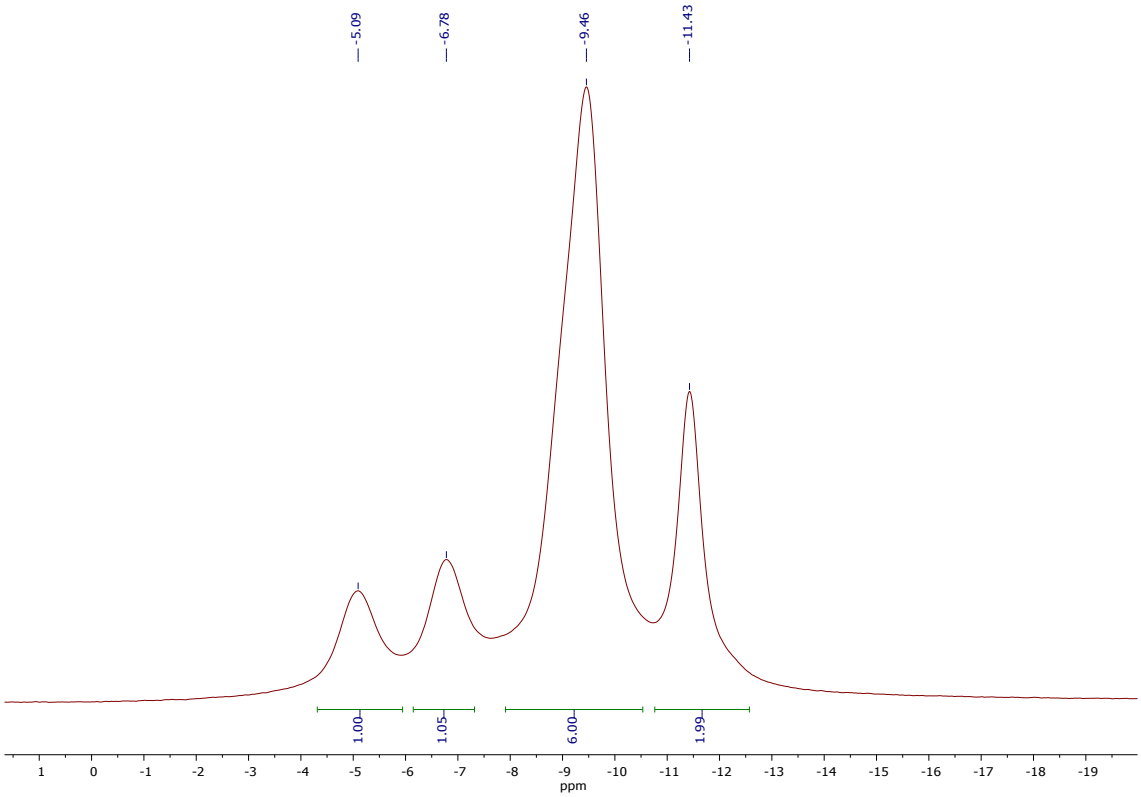

$^{13}C\{^{1}H\}$ NMR (CD_3COCD_3, TMS)

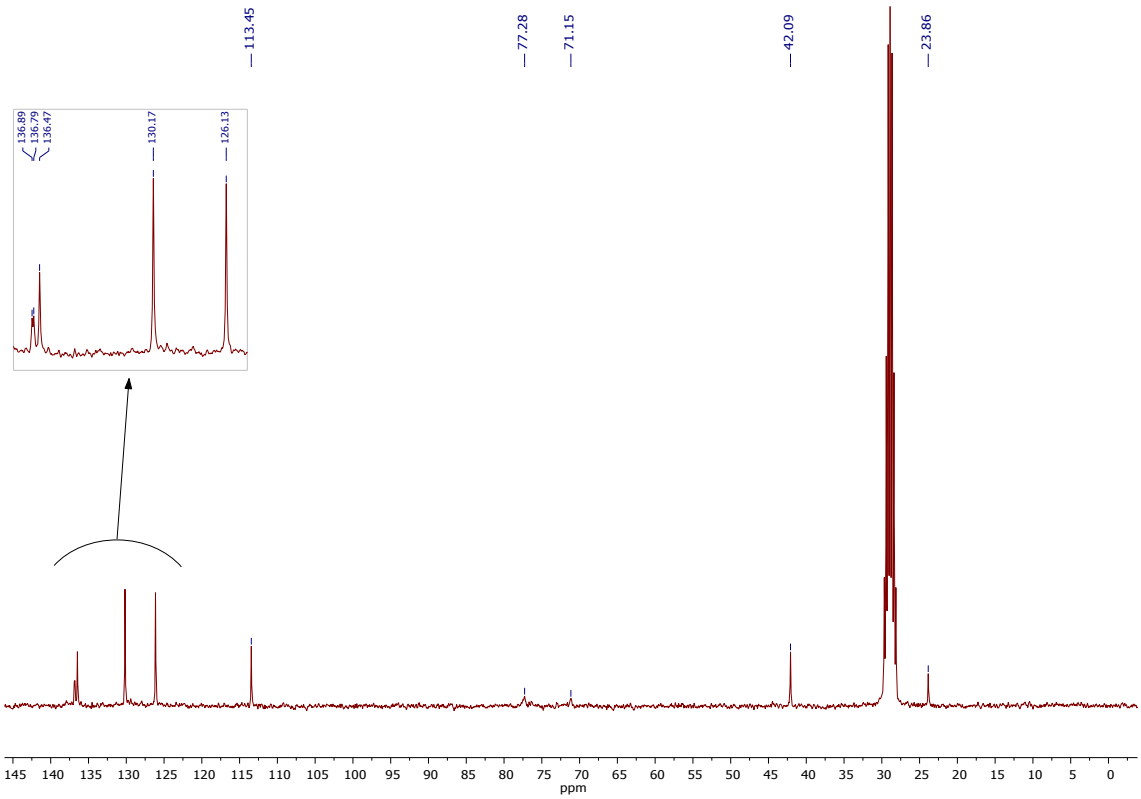

Compound **4**

^{1}H NMR ($CDCl_3$, TMS)

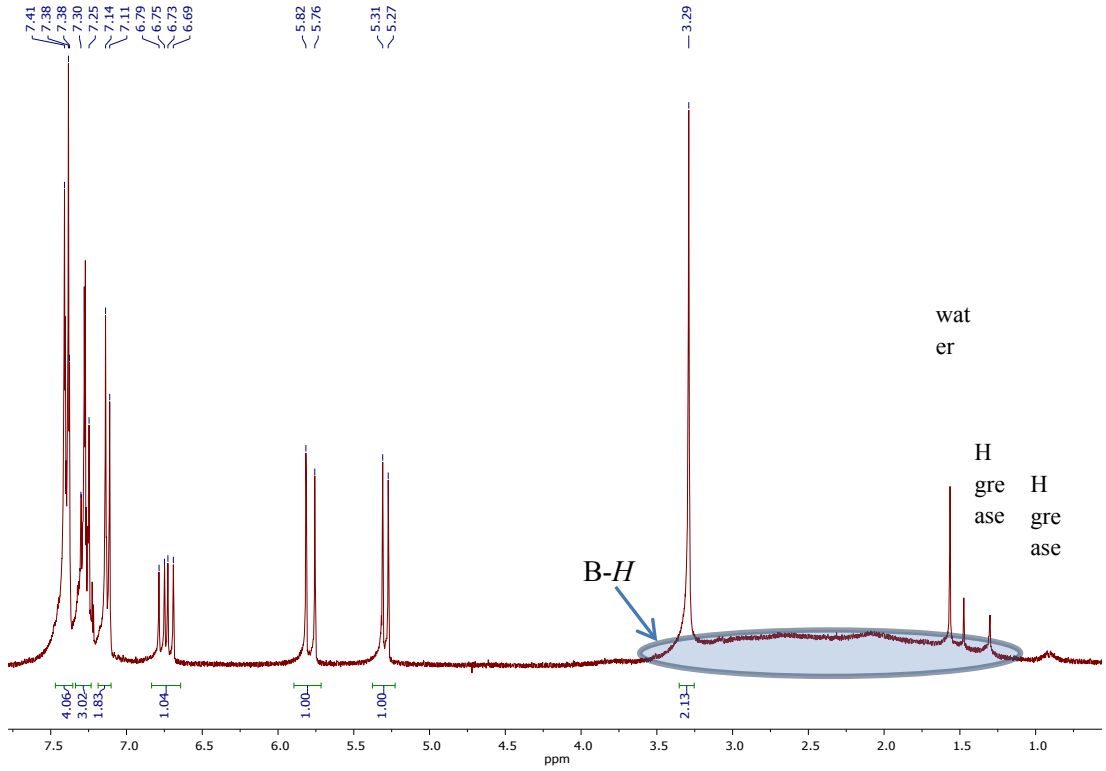

$^{1}H\{^{11}B\}$ NMR ($CDCl_3$, TMS)

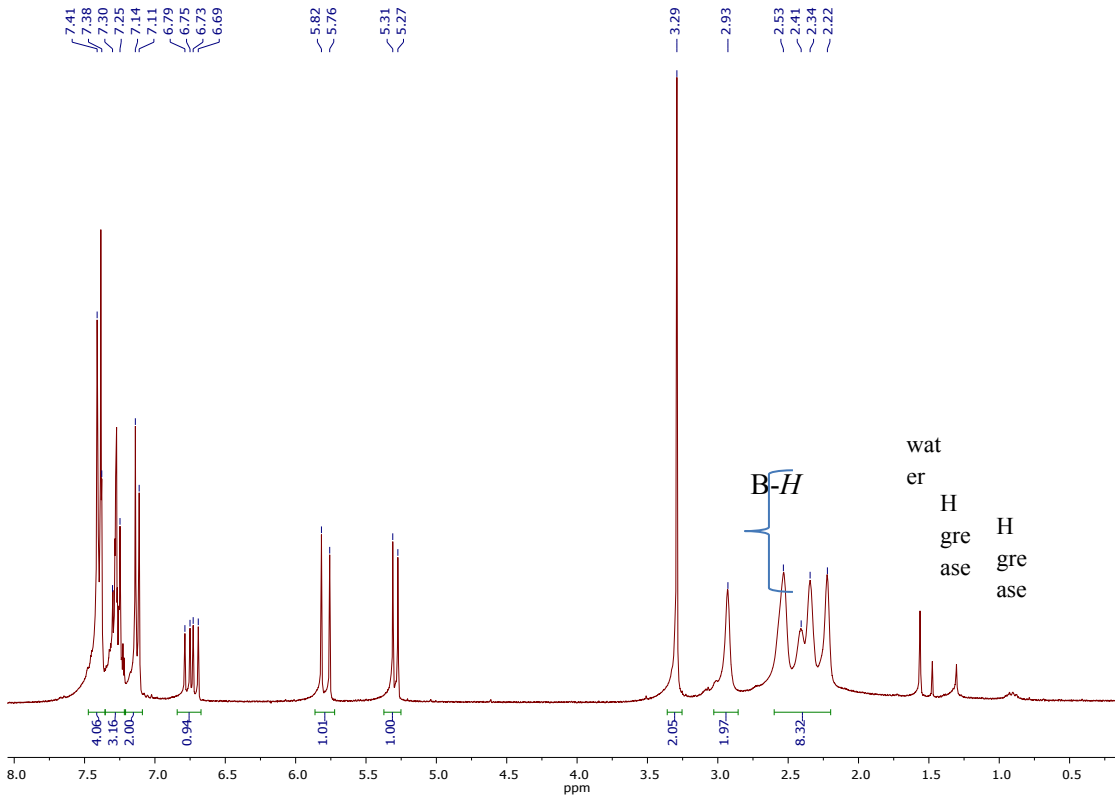

$^{11}B\{^{1}H\}$ NMR ($CDCl_3$, $BF_3 \cdot Et_2O$)

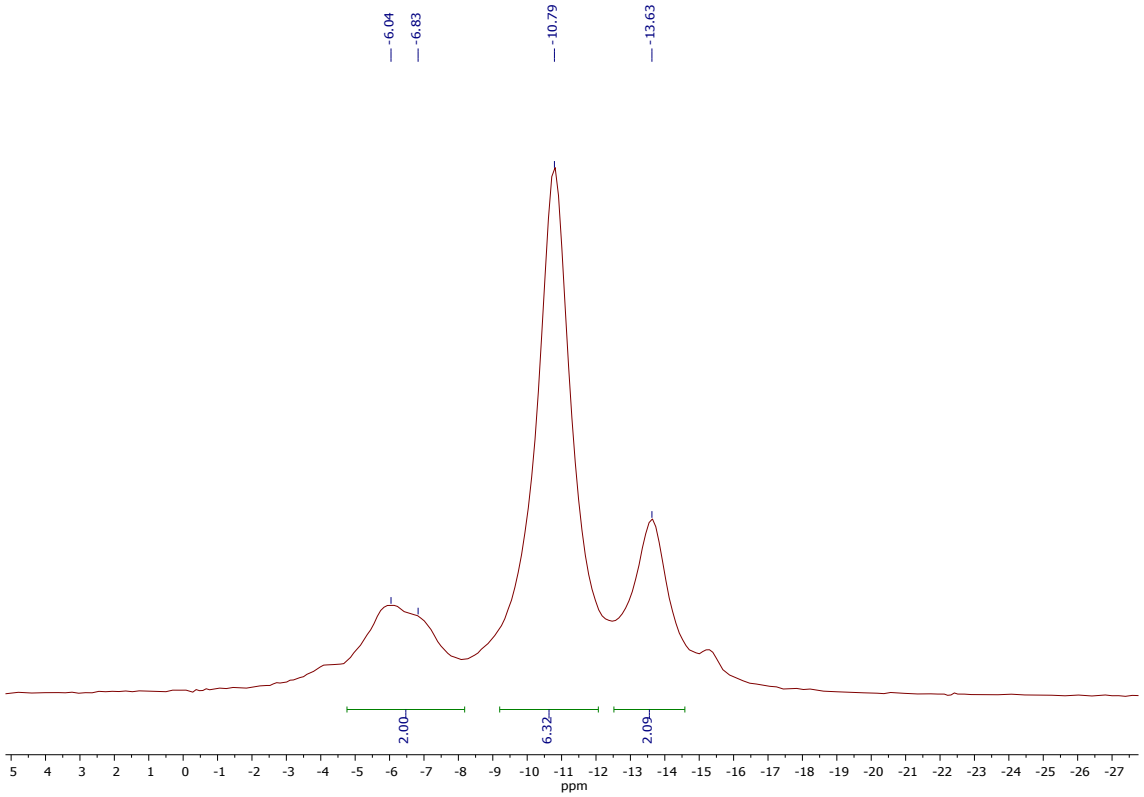

$^{13}C\{^{1}H\}$ NMR ($CDCl_3$, TMS)

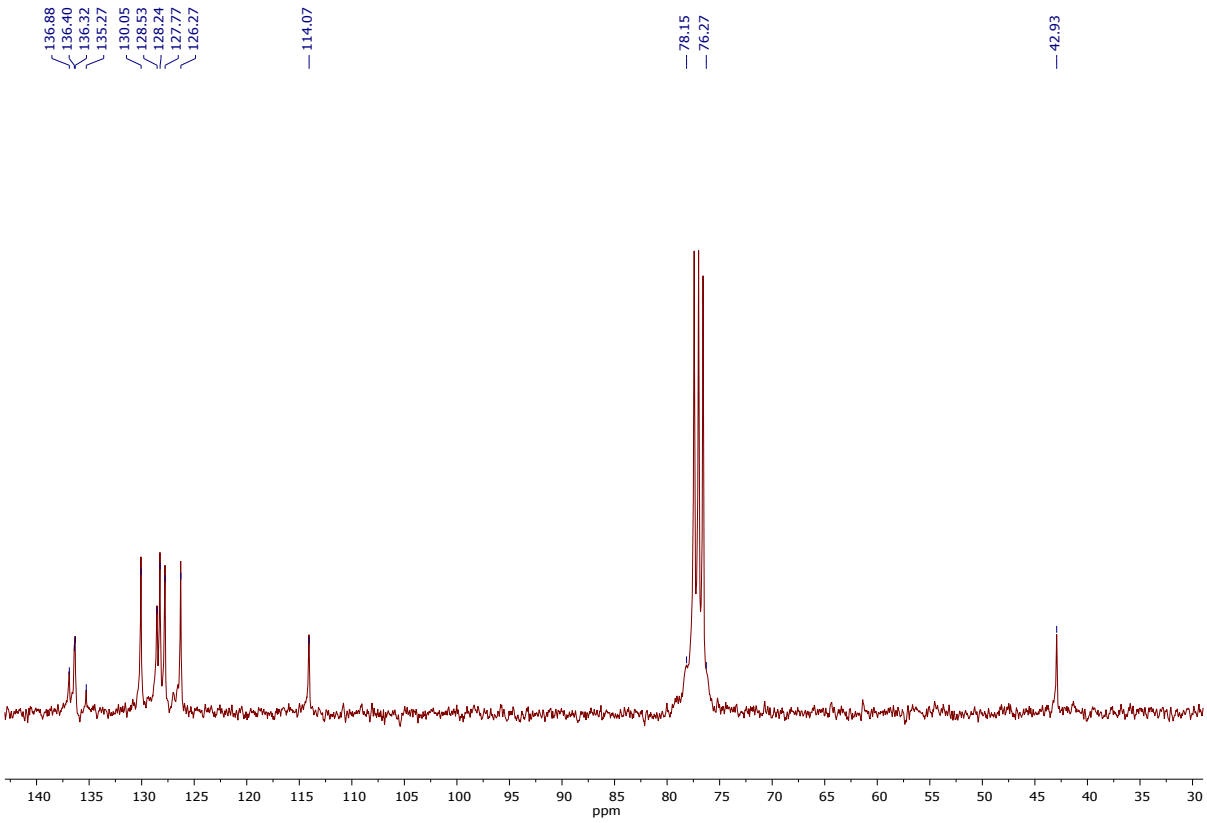

Compound **5**

^{1}H NMR ($CDCl_3$, TMS)

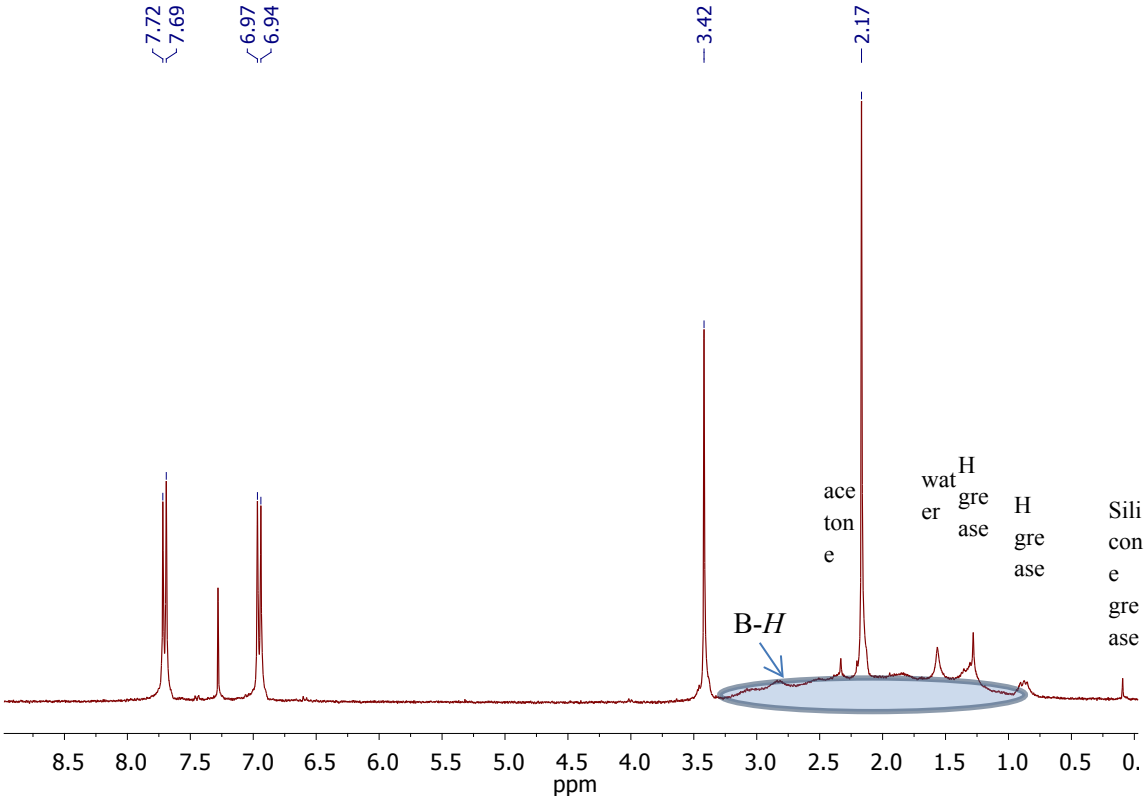

$^{1}H\{^{11}B\}$ NMR ($CDCl_3$, TMS)

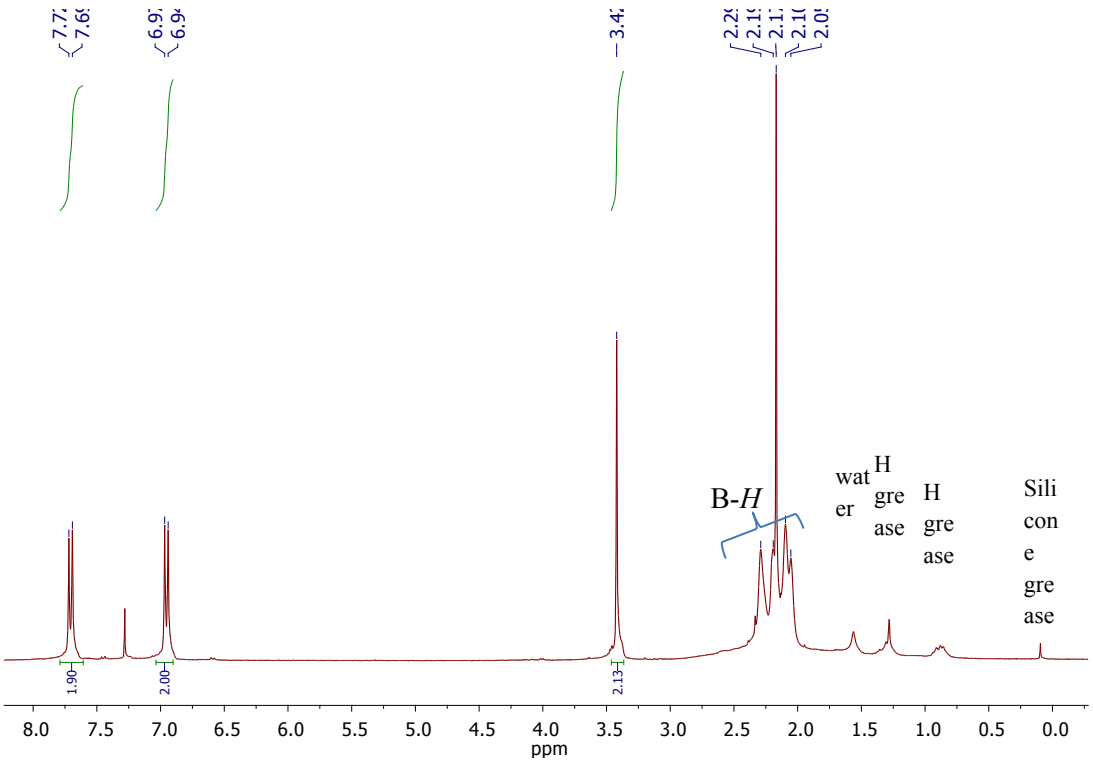

$^{11}B\{^{1}H\}$ NMR ($CDCl_3$, $BF_3 \cdot Et_2O$)

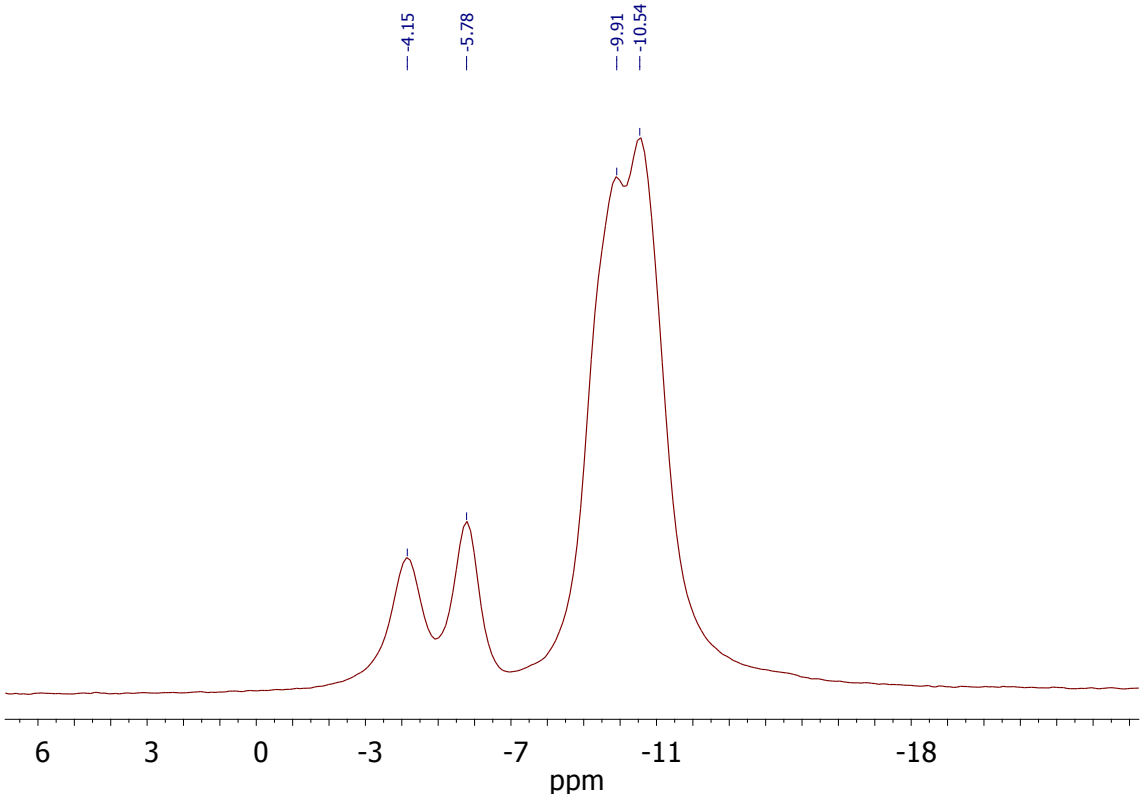

$^{13}C\{^{1}H\}$ NMR ($CDCl_3$, TMS)

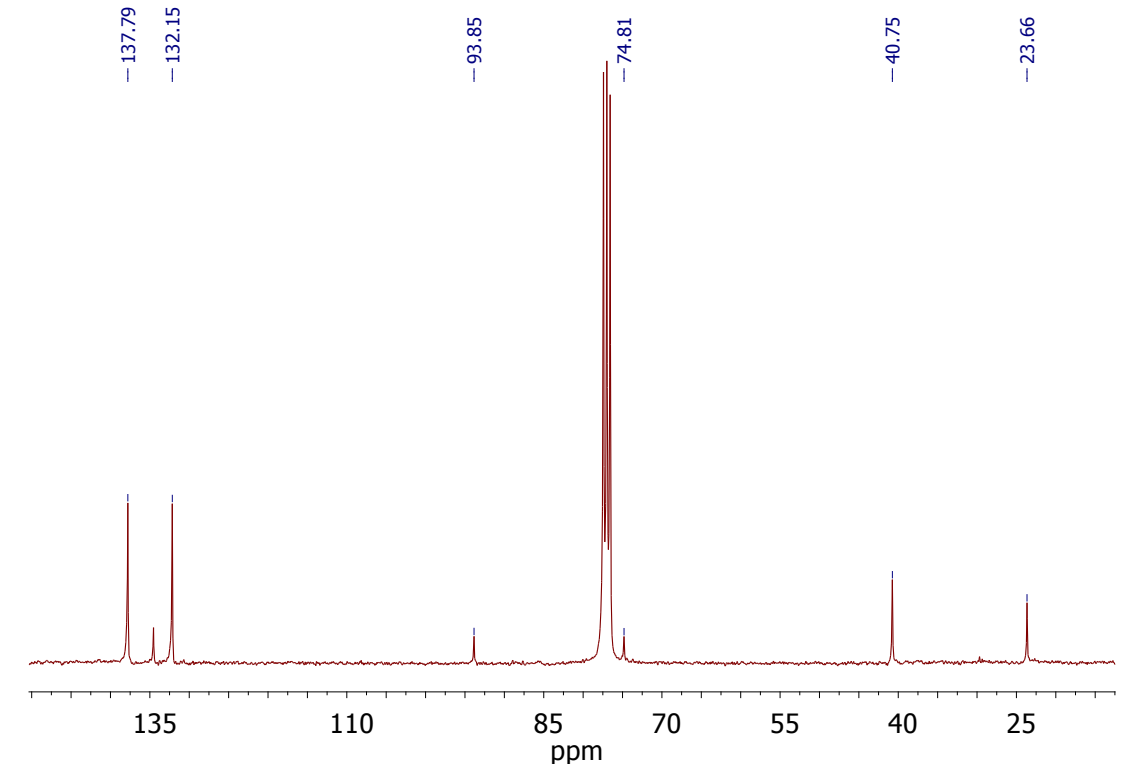

Compound **6**

^{1}H NMR ($CDCl_3$, TMS)

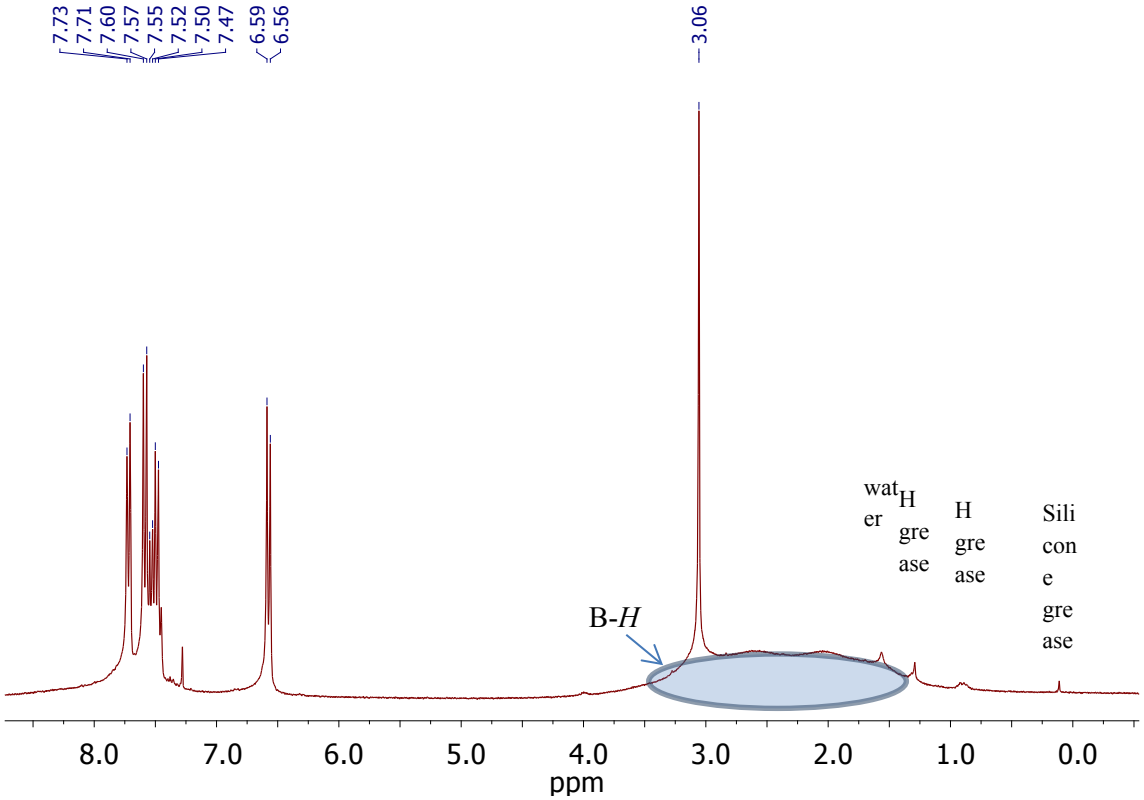

$^{1}H\{^{11}B\}$ NMR ($CDCl_3$, TMS)

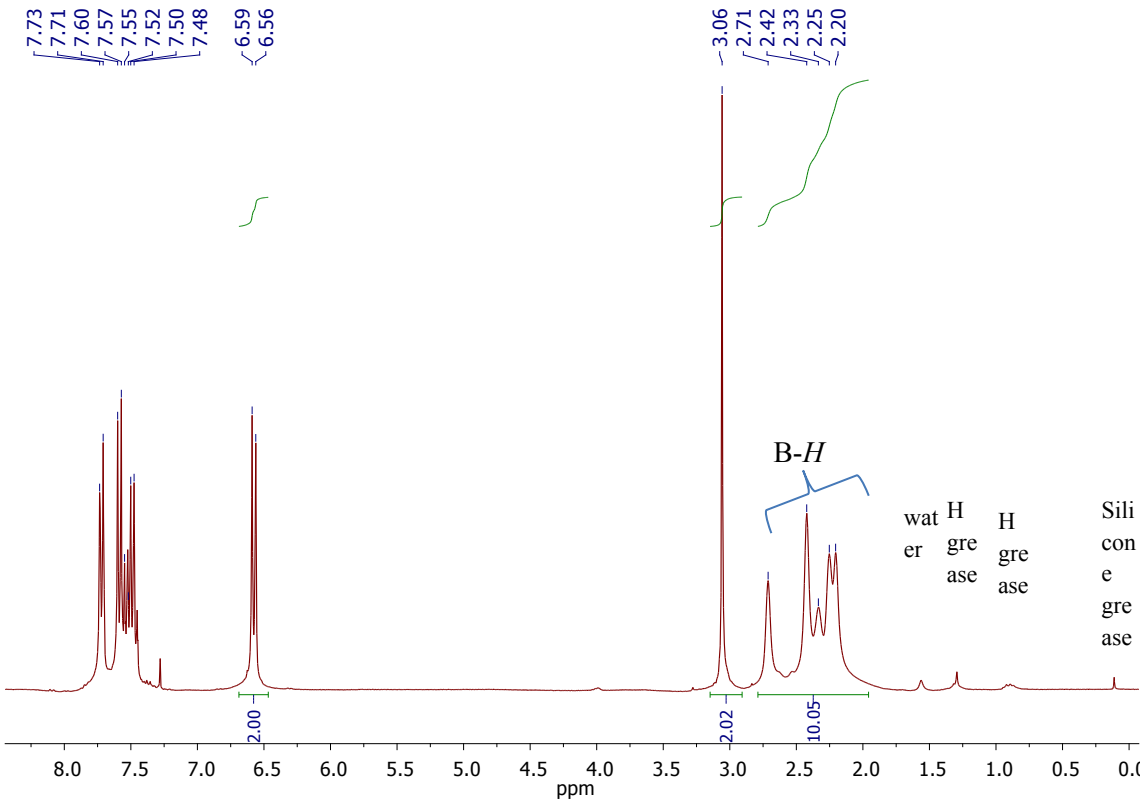

$^{11}B\{^{1}H\}$ NMR ($CDCl_3$, $BF_3 \cdot Et_2O$)

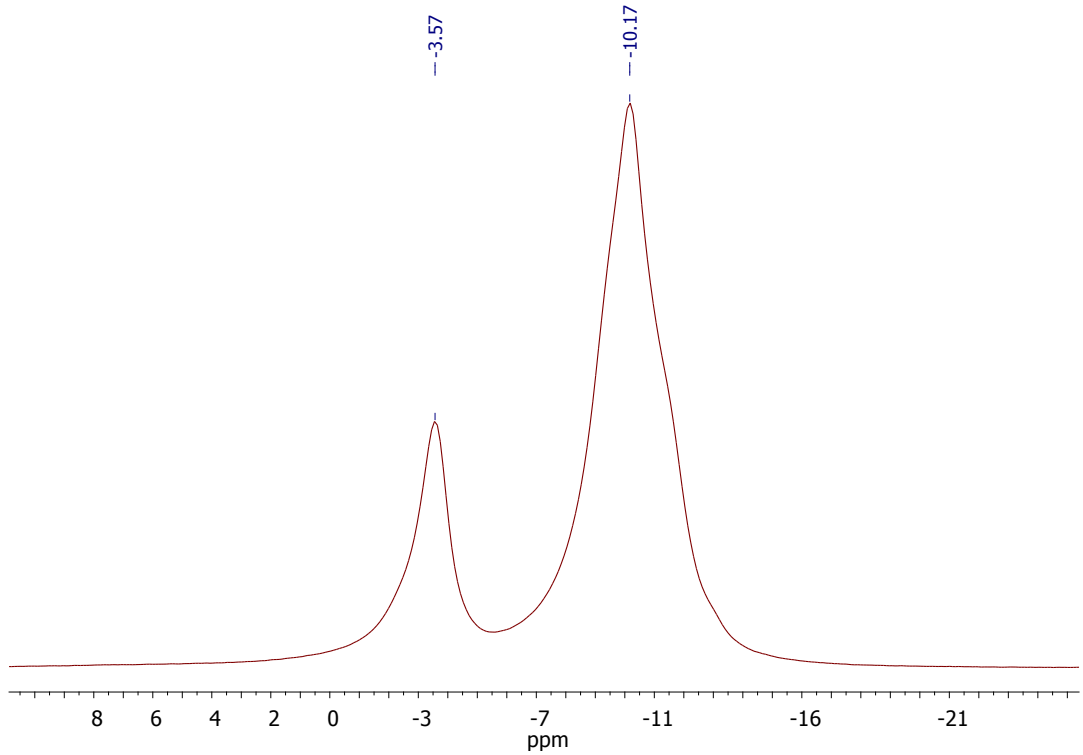

$^{13}C\{^{1}H\}$ NMR ($CDCl_3$, TMS)

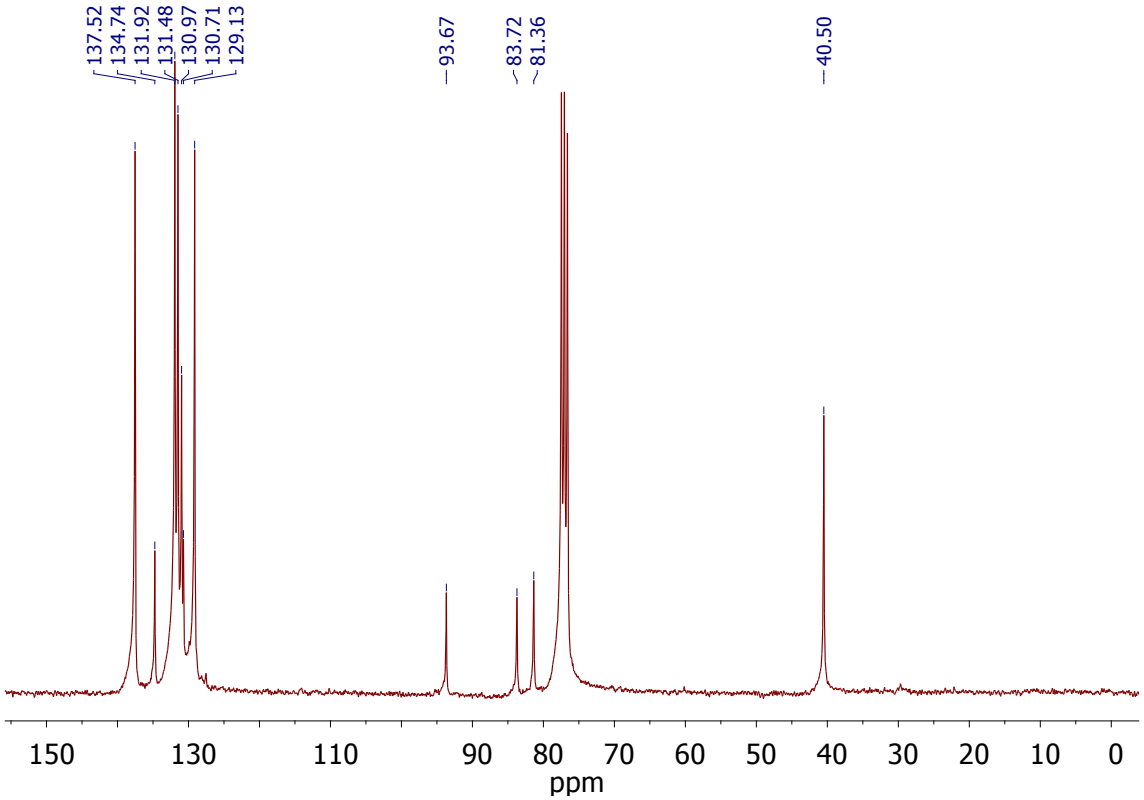

Compound **7**

^{1}H NMR ($CDCl_3$, TMS)

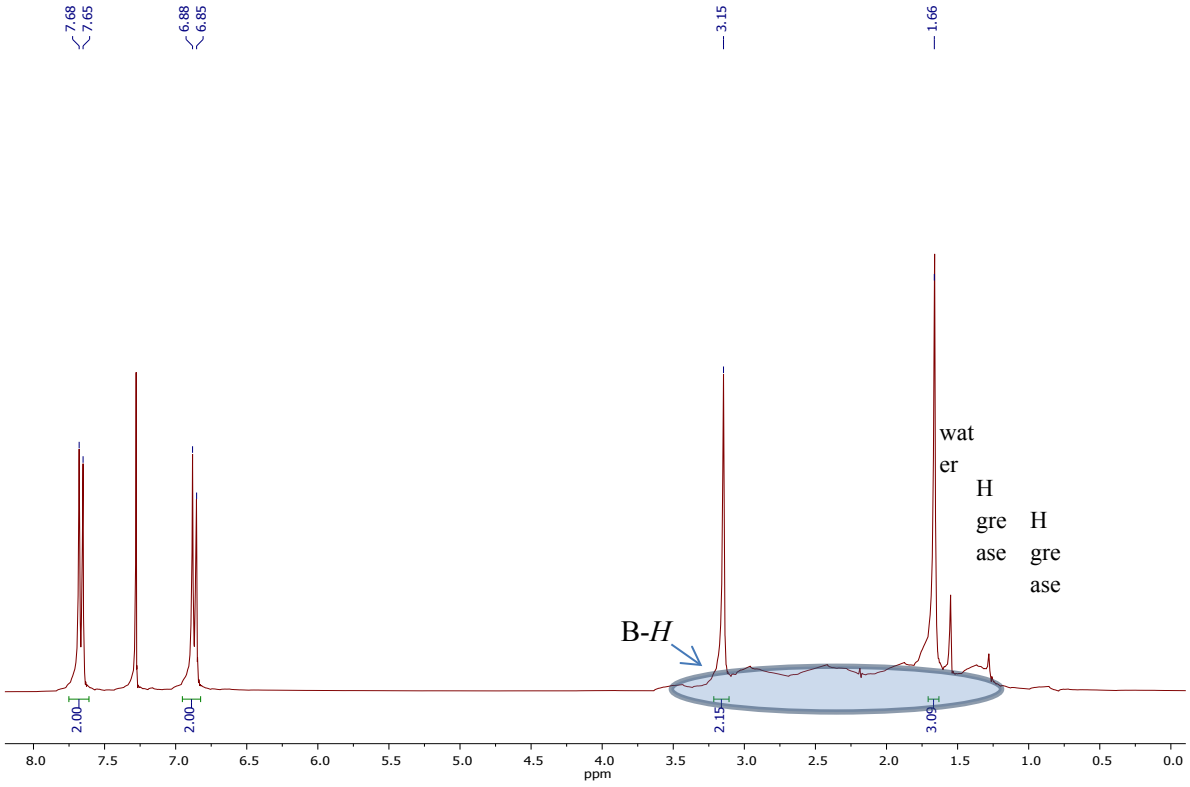

$^{1}H\{^{11}B\}$ NMR ($CDCl_3$, TMS)

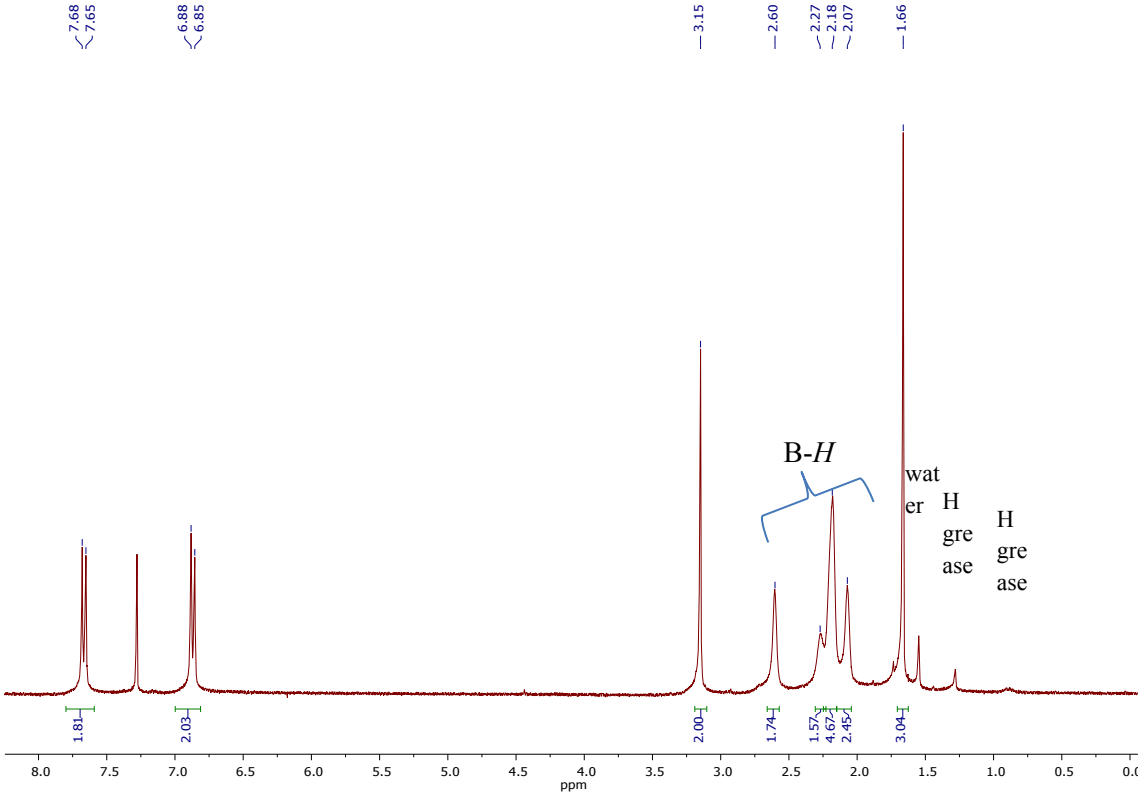

$^{11}B\{^{1}H\}$ NMR ($CDCl_3$, $BF_3 \cdot Et_2O$)

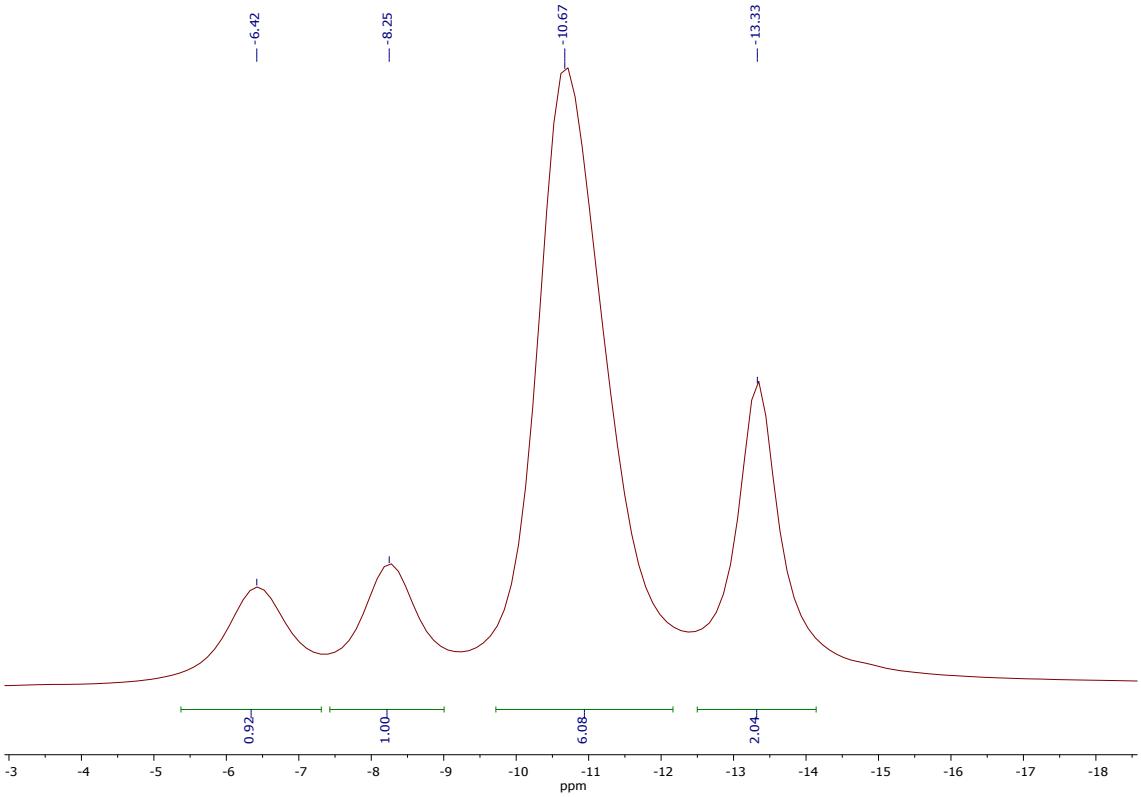

$^{13}C\{^{1}H\}$ NMR ($CDCl_3$, TMS)

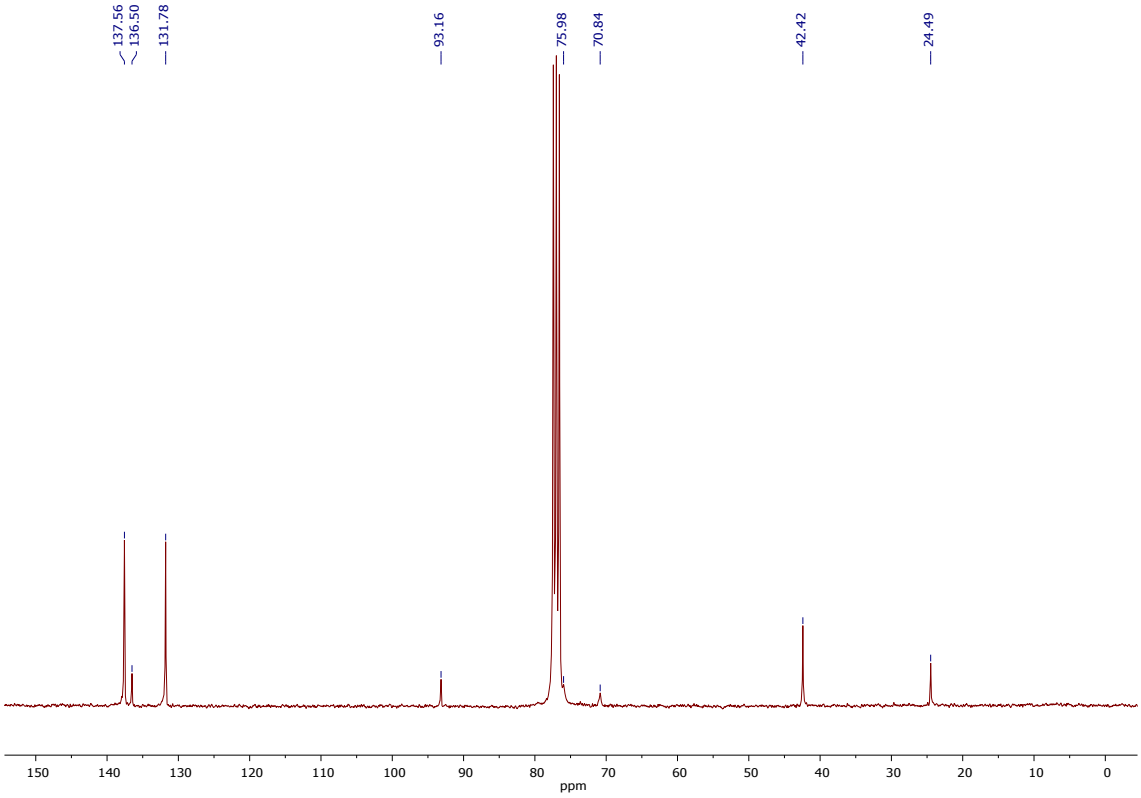

Compound 8

^{1}H NMR ($CDCl_3$, TMS)

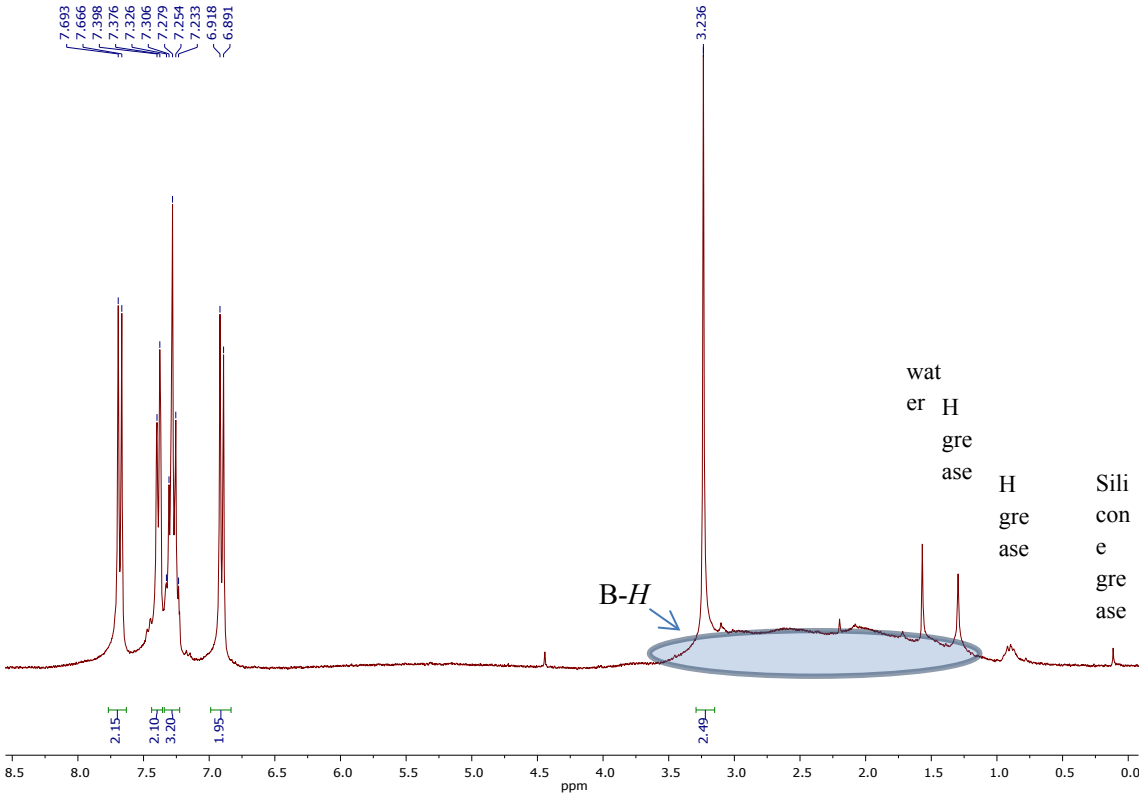

$^{1}H\{^{11}B\}$ NMR ($CDCl_3$, TMS)

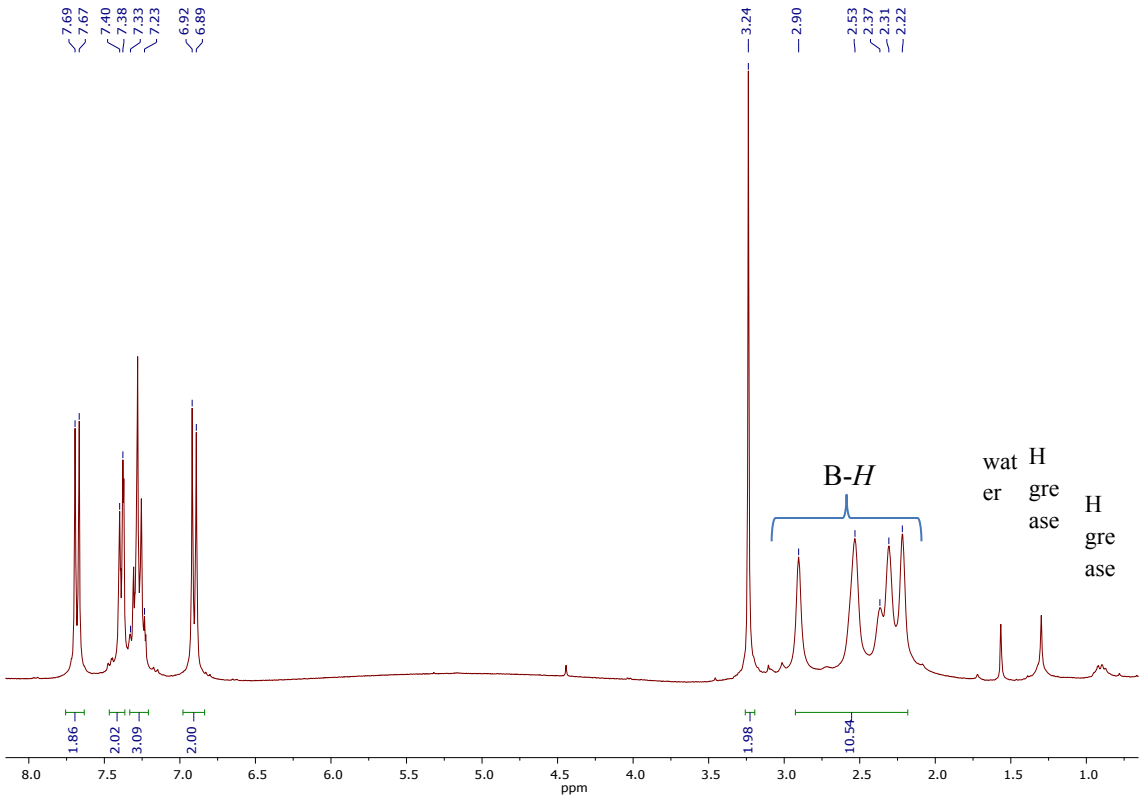

$^{11}B\{^{1}H\}$ NMR ($CDCl_3$, $BF_3 \cdot Et_2O$)

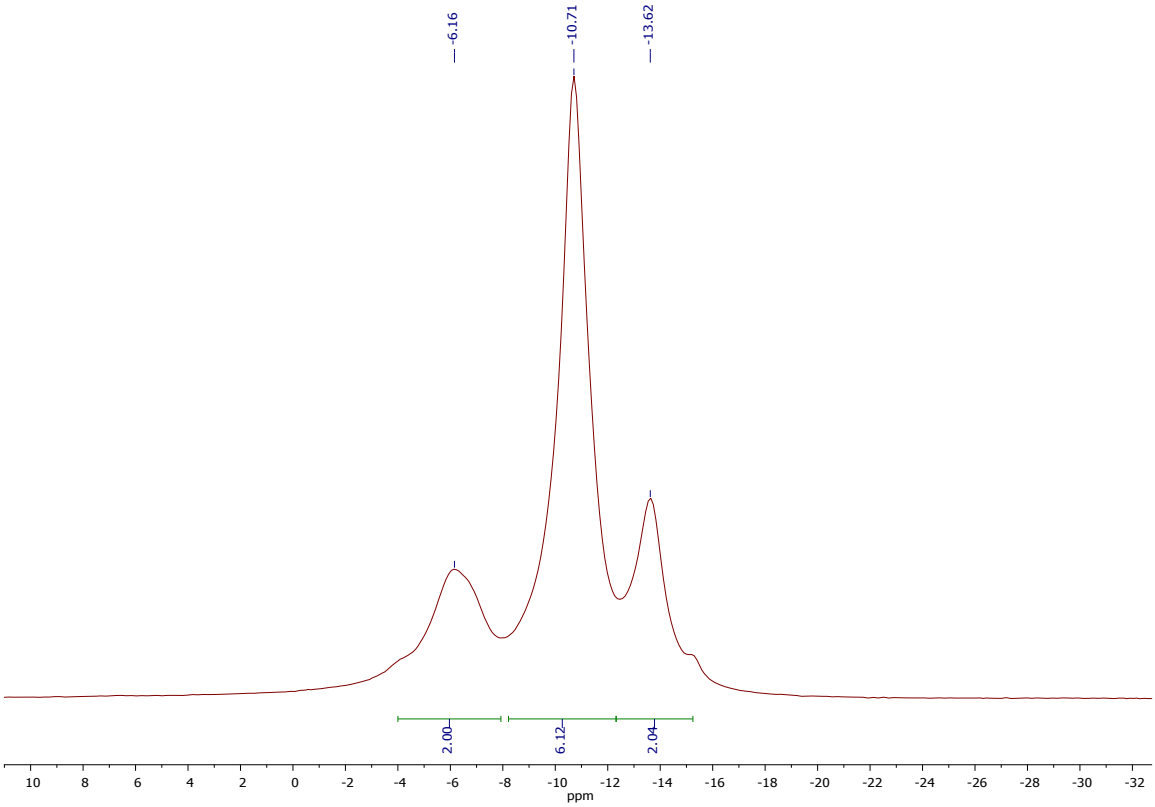

$^{13}C\{^{1}H\}$ NMR ($CDCl_3$, TMS)

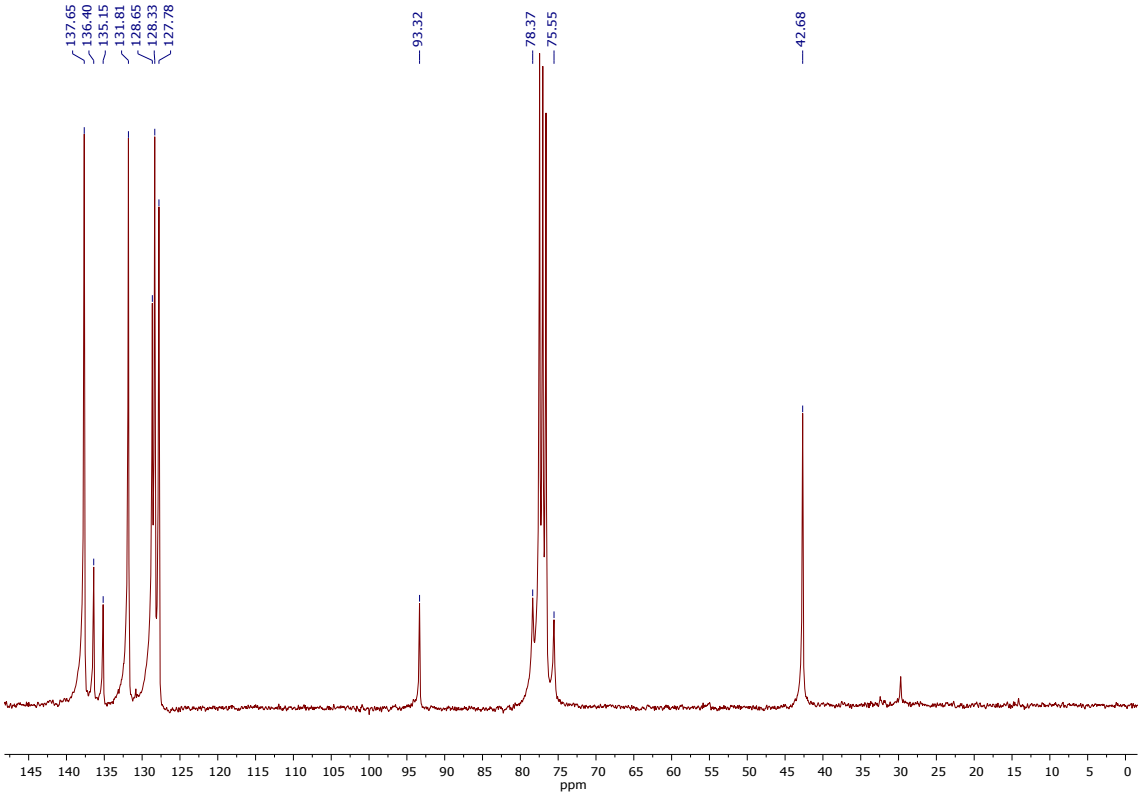

Compound **9**

^{1}H NMR ($CDCl_3$, TMS)

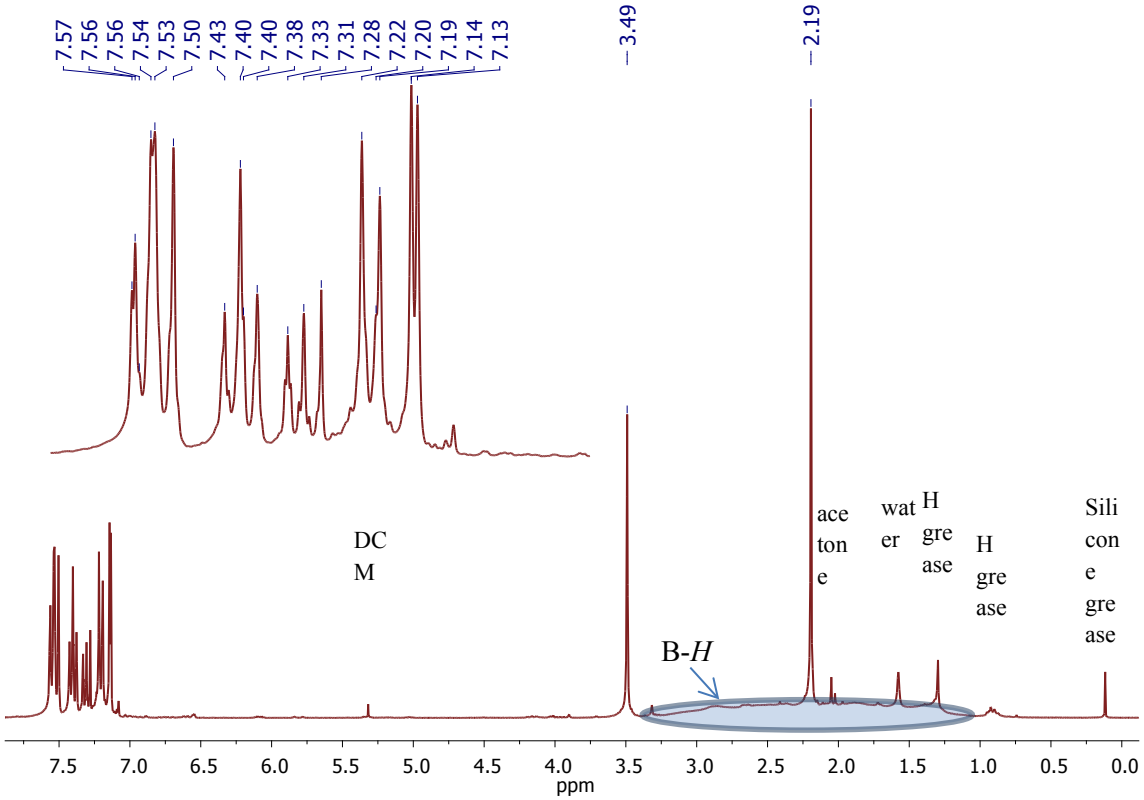

$^{1}H\{^{11}B\}$ NMR ($CDCl_3$, TMS)

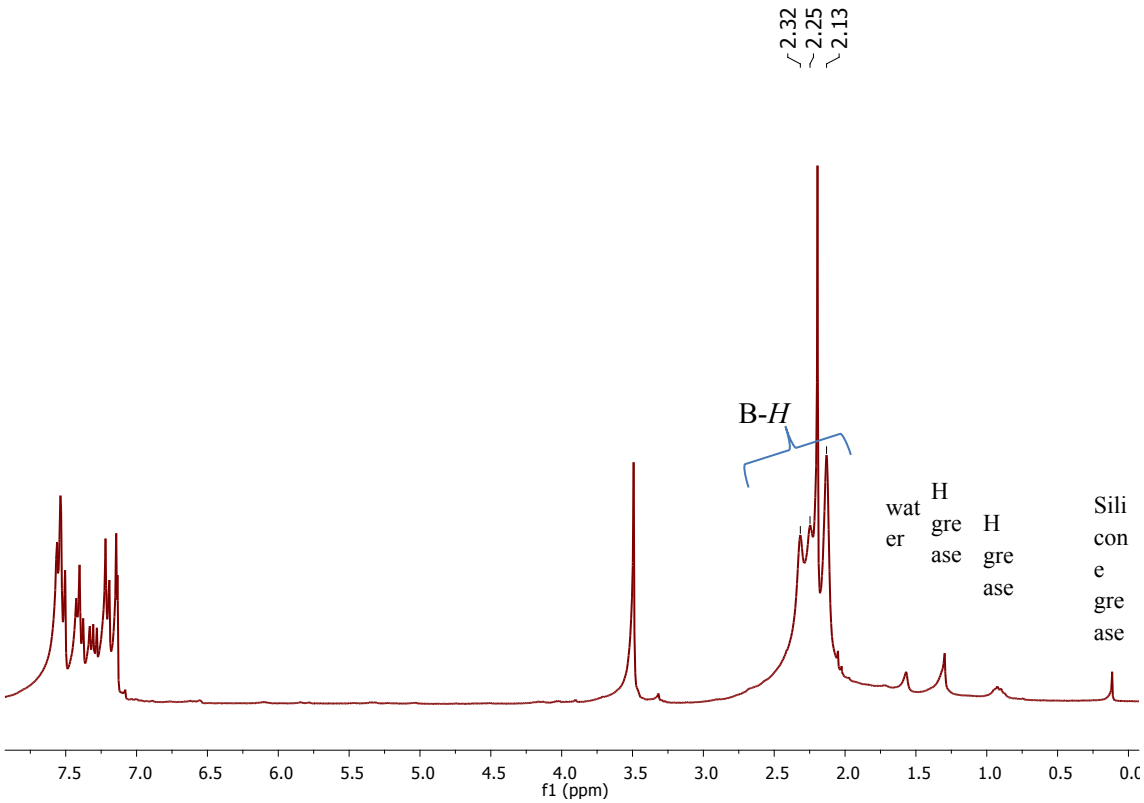

$^{11}B\{^{1}H\}$ NMR ($CDCl_3$, $BF_3 \cdot Et_2O$)

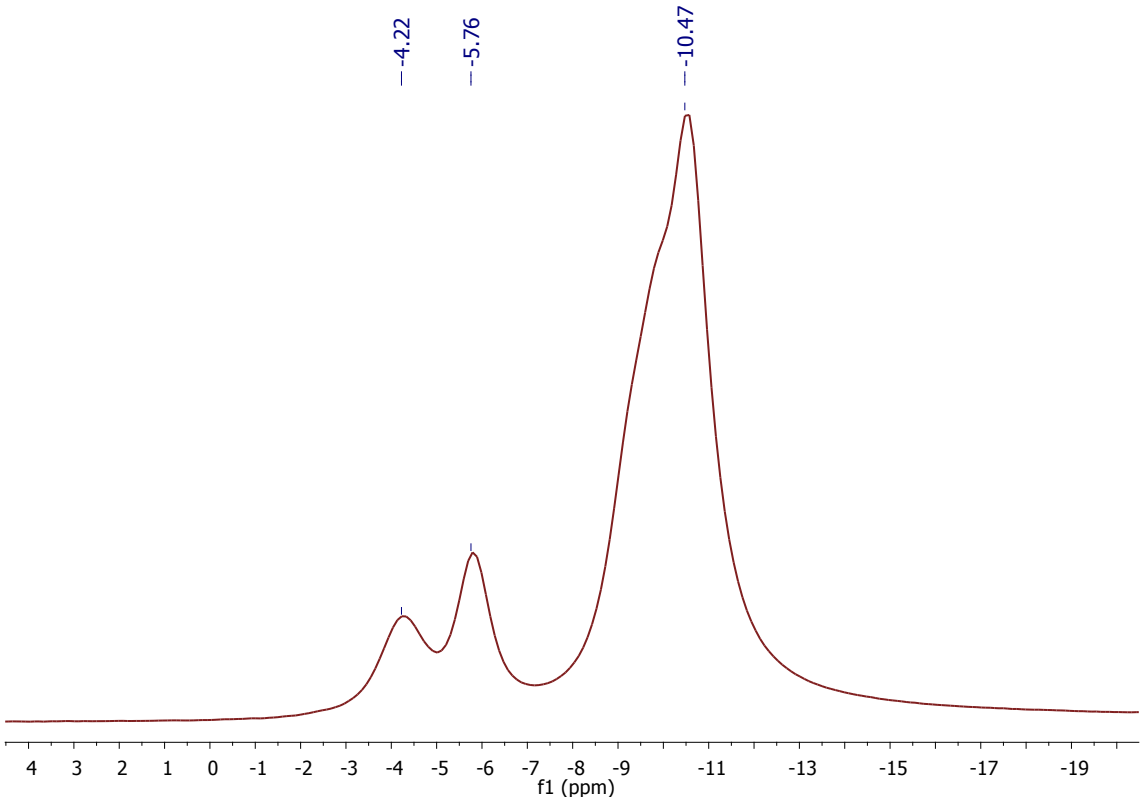

$^{13}C\{^{1}H\}$ NMR ($CDCl_3$, TMS)

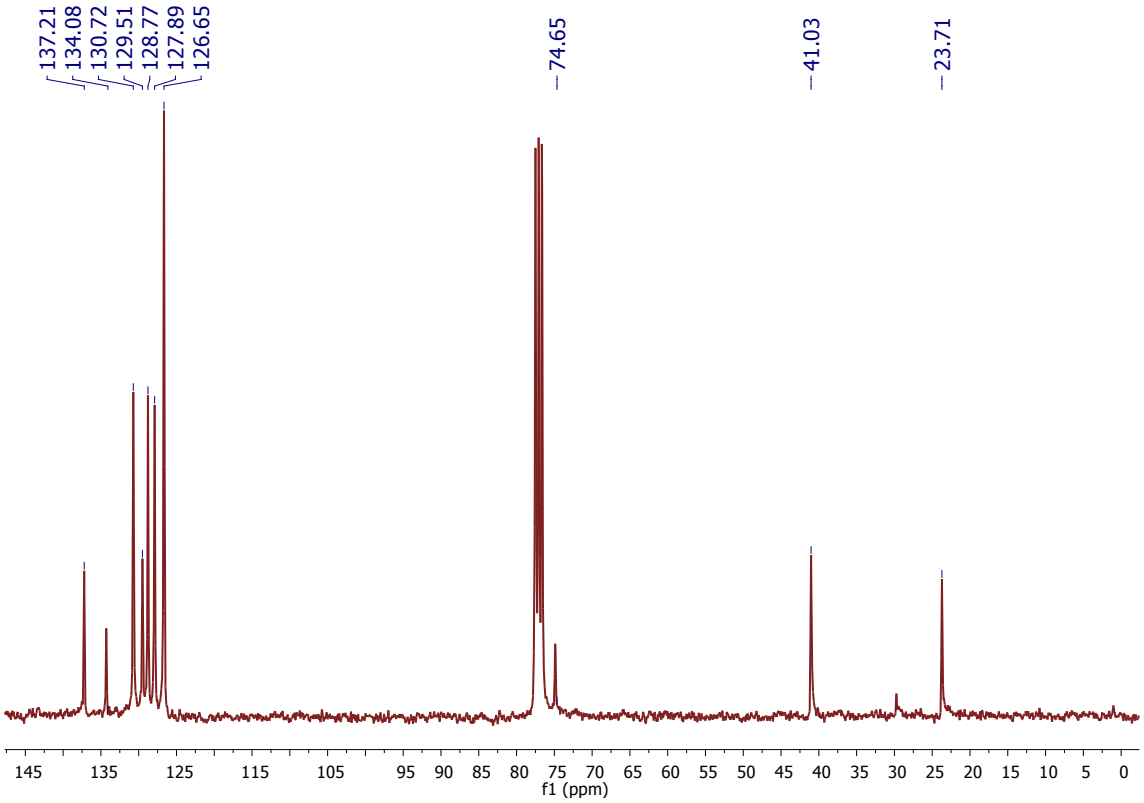

Compound **10**

^{1}H NMR ($CDCl_3$, TMS)

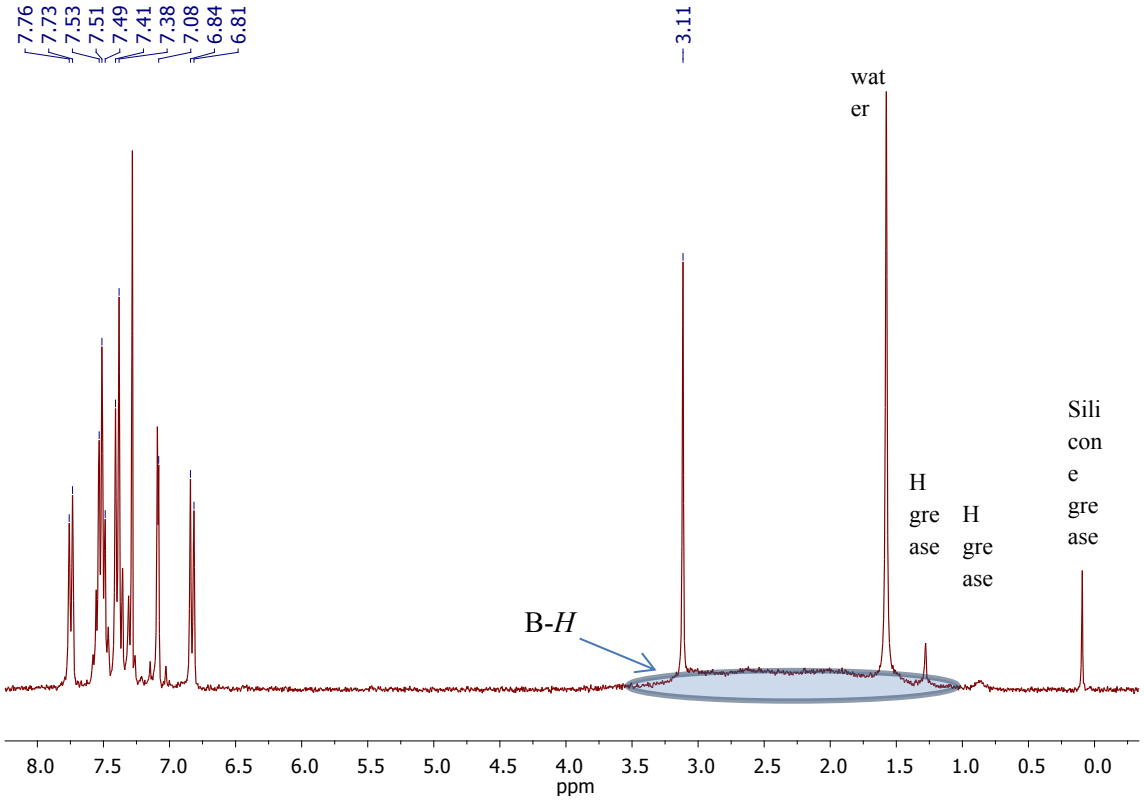

$^{1}H\{^{11}B\}$ NMR ($CDCl_3$, TMS)

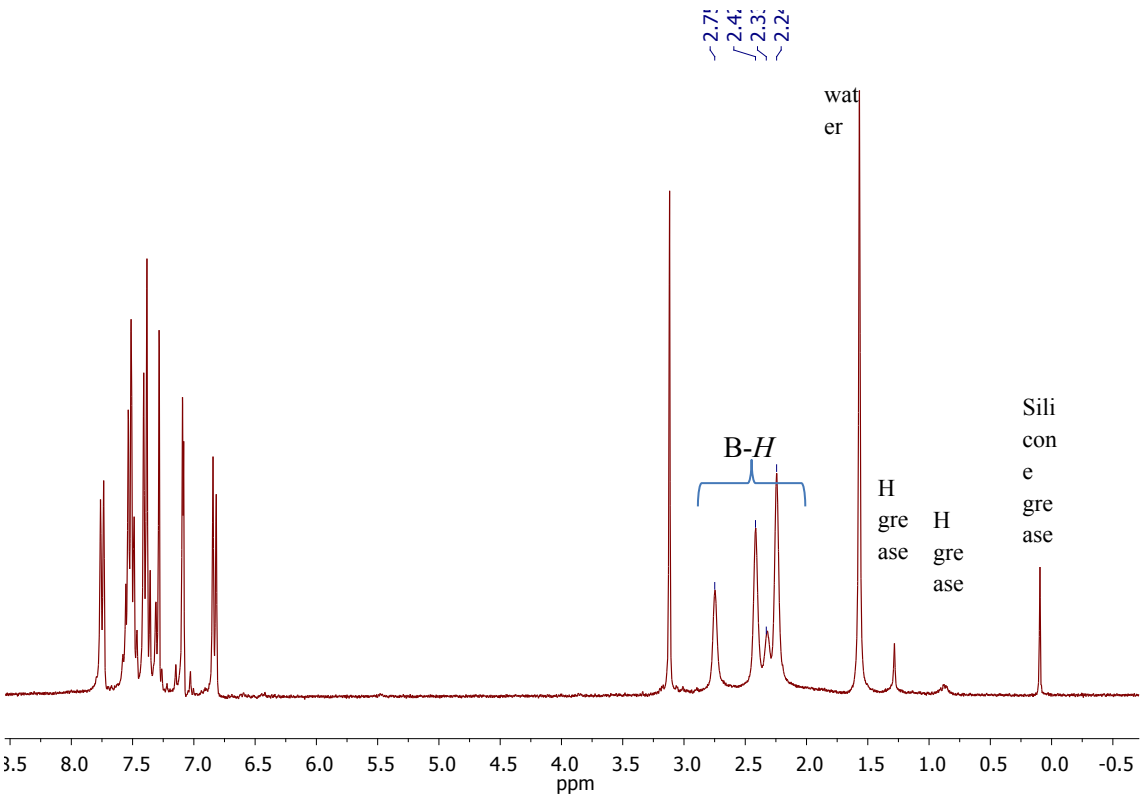

$^{11}B\{^{1}H\}$ NMR ($CDCl_3$, $BF_3 \cdot Et_2O$)

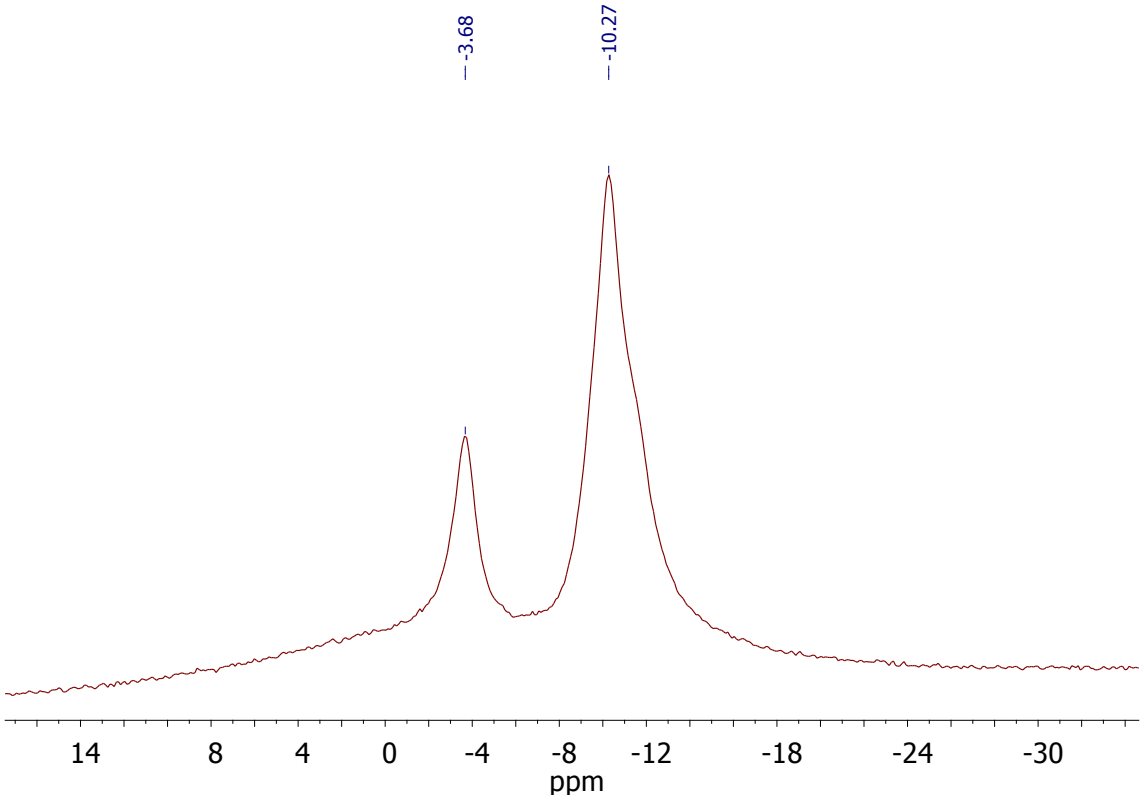

Compound **11**

^{1}H NMR ($CDCl_3$, TMS)

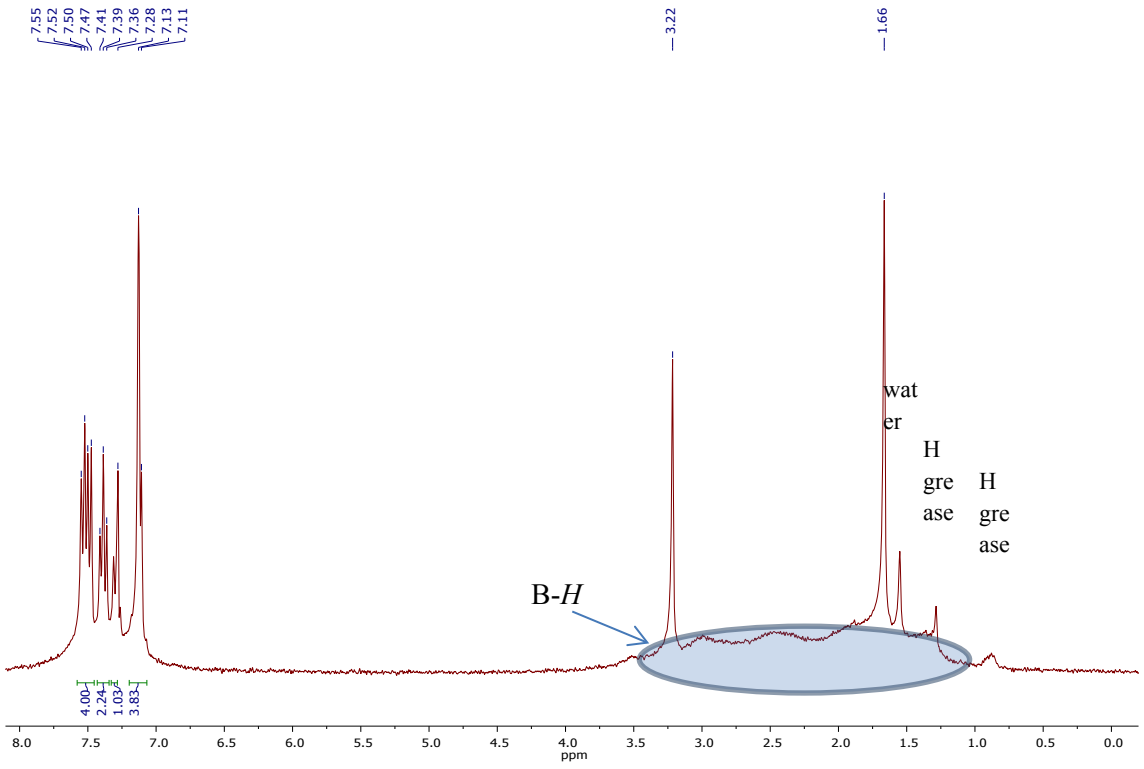

$^{1}H\{^{11}B\}$ NMR ($CDCl_3$, TMS)

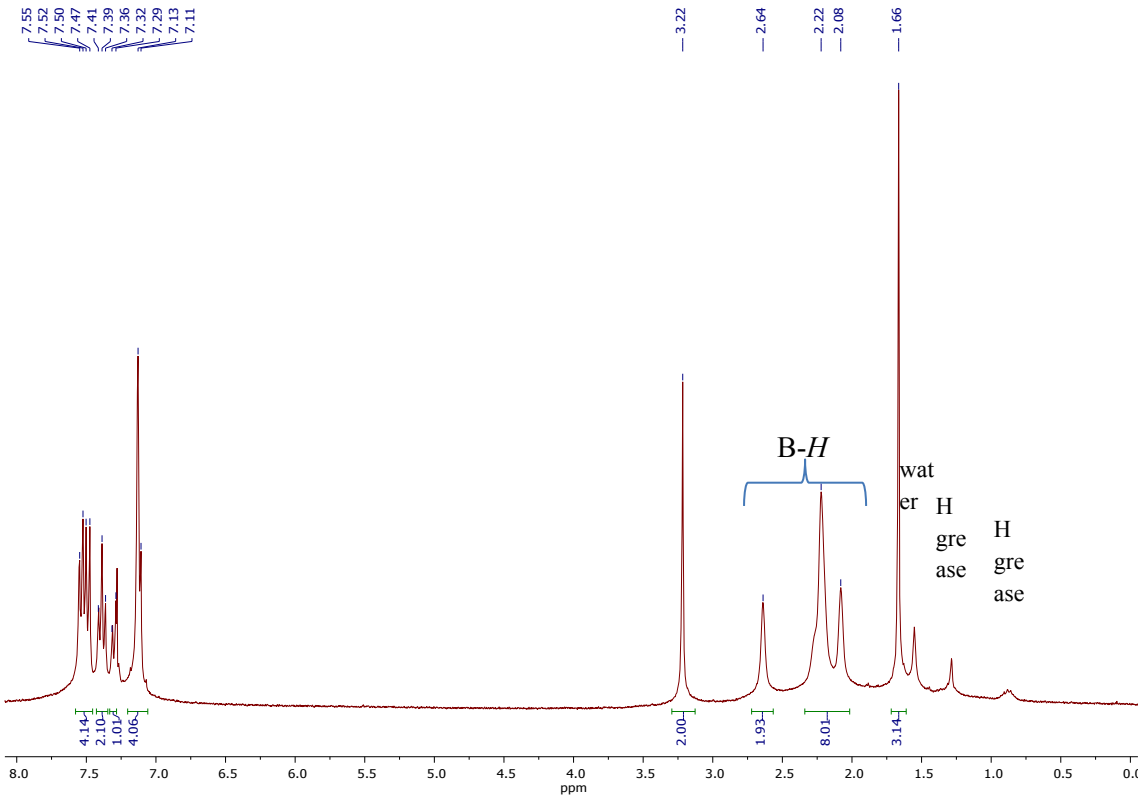

$^{11}B\{^{1}H\}$ NMR ($CDCl_3$, $BF_3{\cdot}Et_2O$)

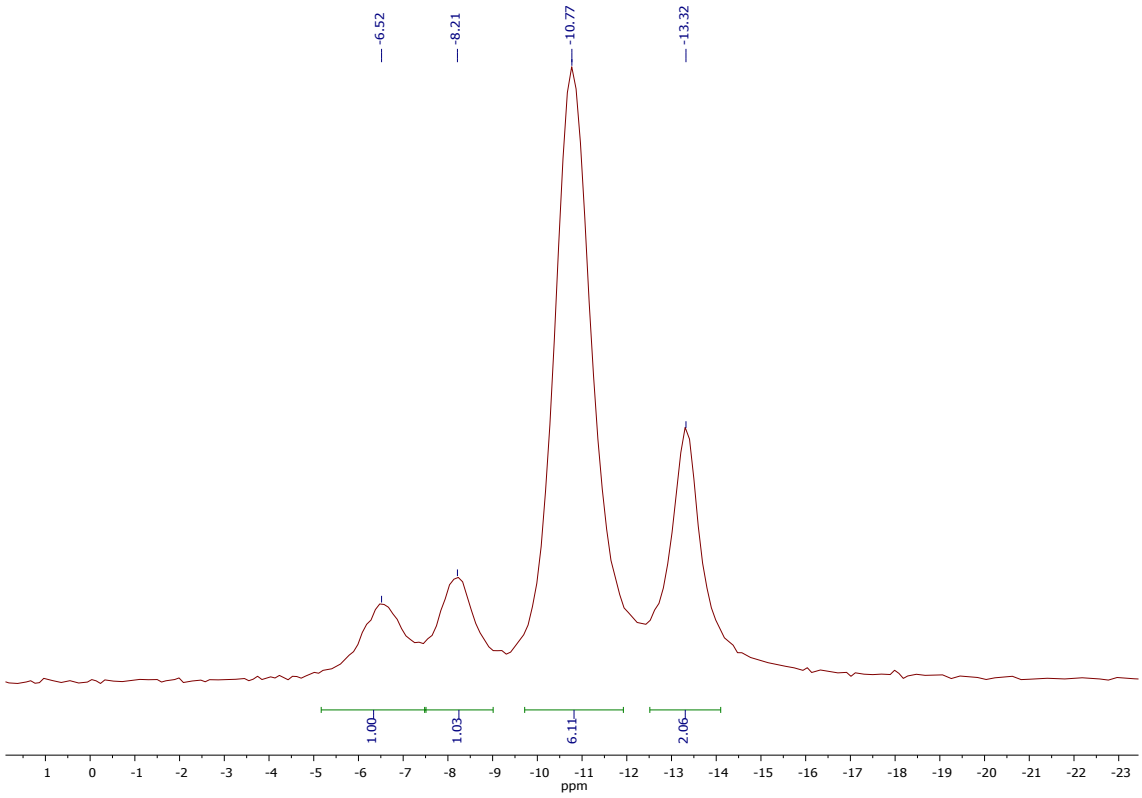

$^{13}C\{^{1}H\}$ NMR ($CDCl_3$, TMS)

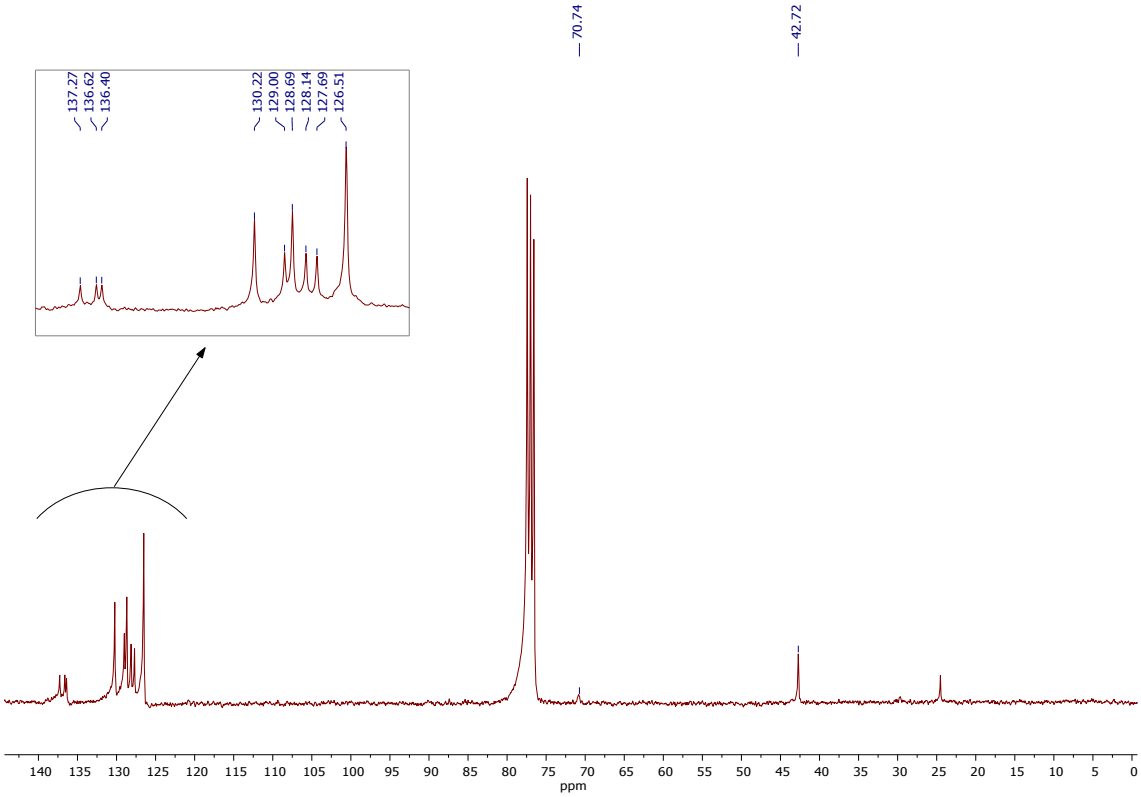

Compound **12**

^{1}H NMR ($CDCl_3$, TMS)

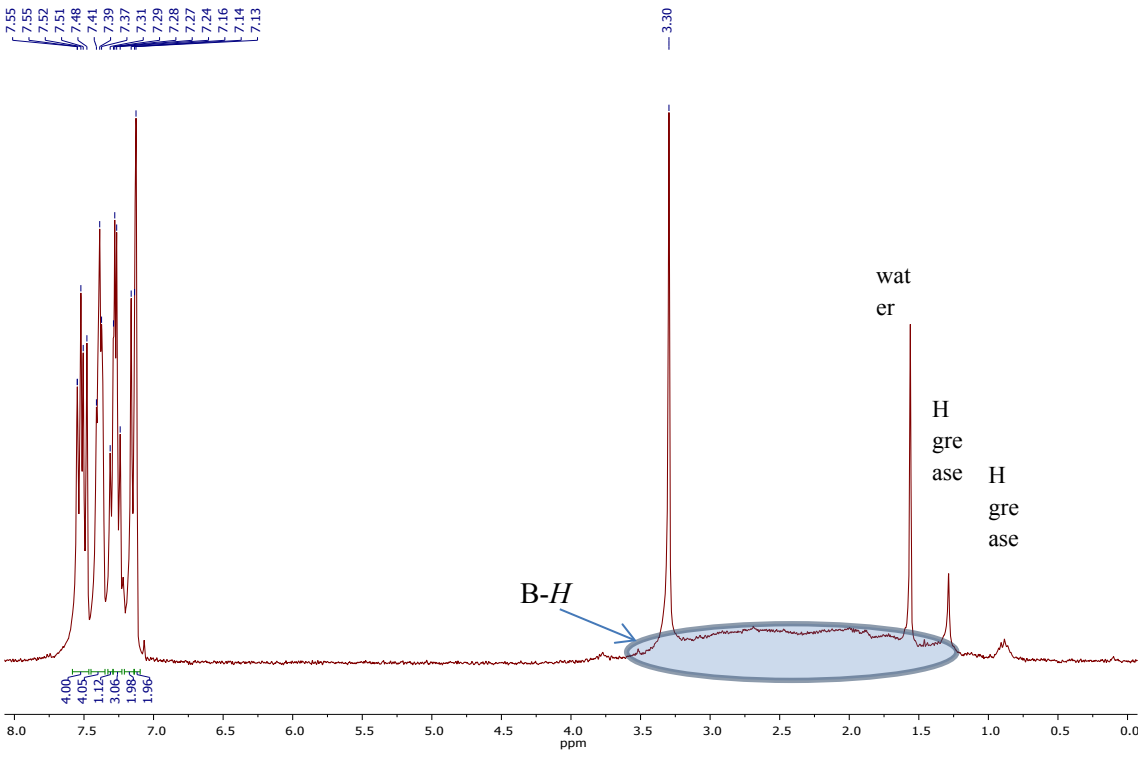

$^{1}H\{^{11}B\}$ NMR ($CDCl_3$, TMS)

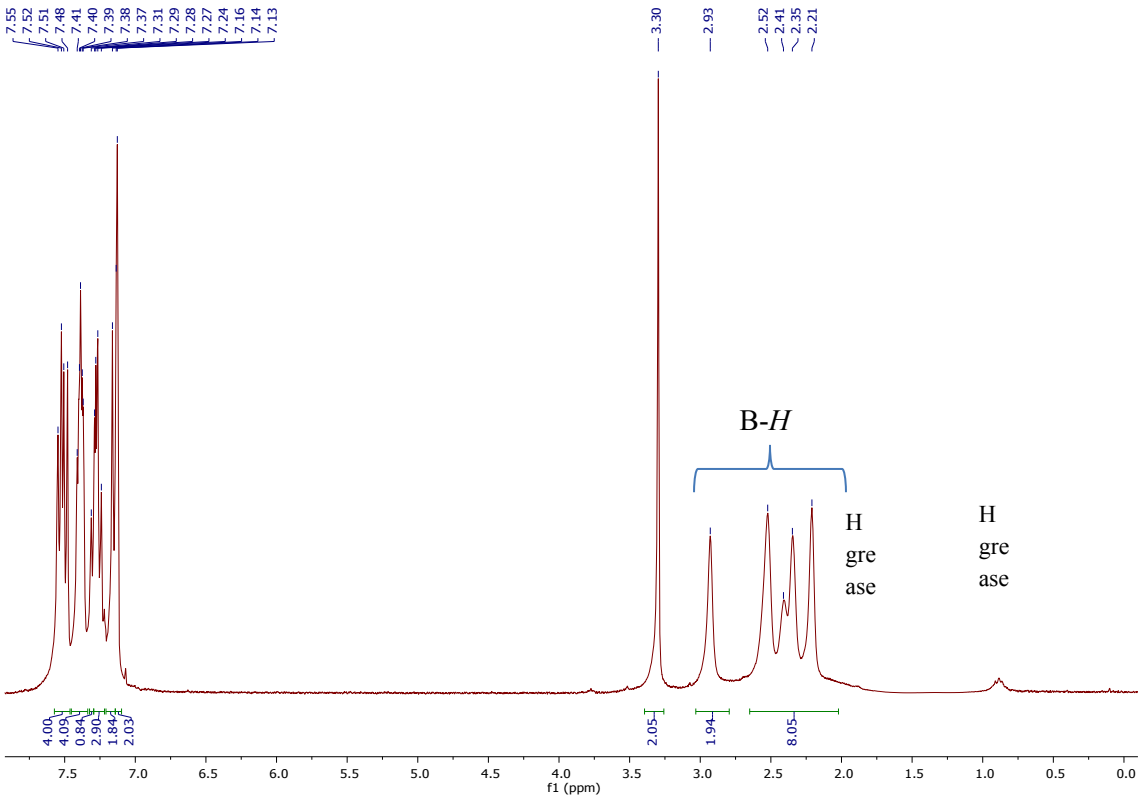

$^{11}B\{^{1}H\}$ NMR ($CDCl_3$, $BF_3 \cdot Et_2O$)

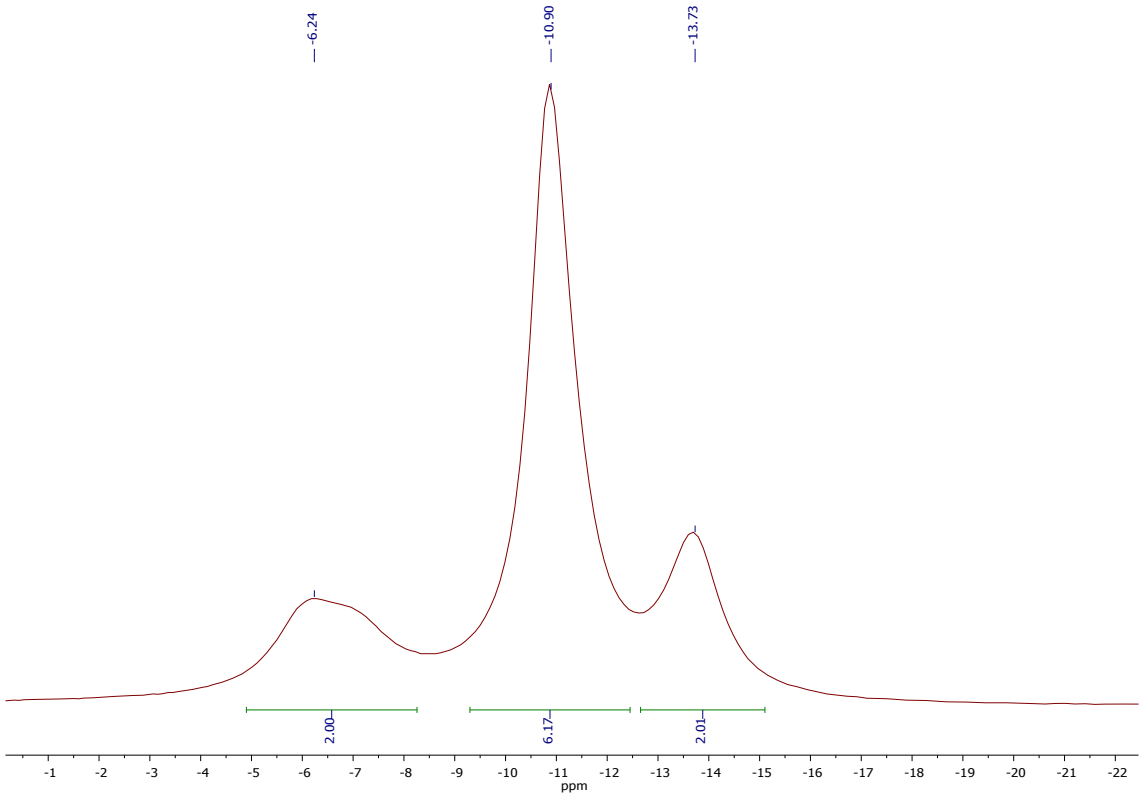

$^{13}C\{^{1}H\}$ NMR ($CDCl_3$, TMS)

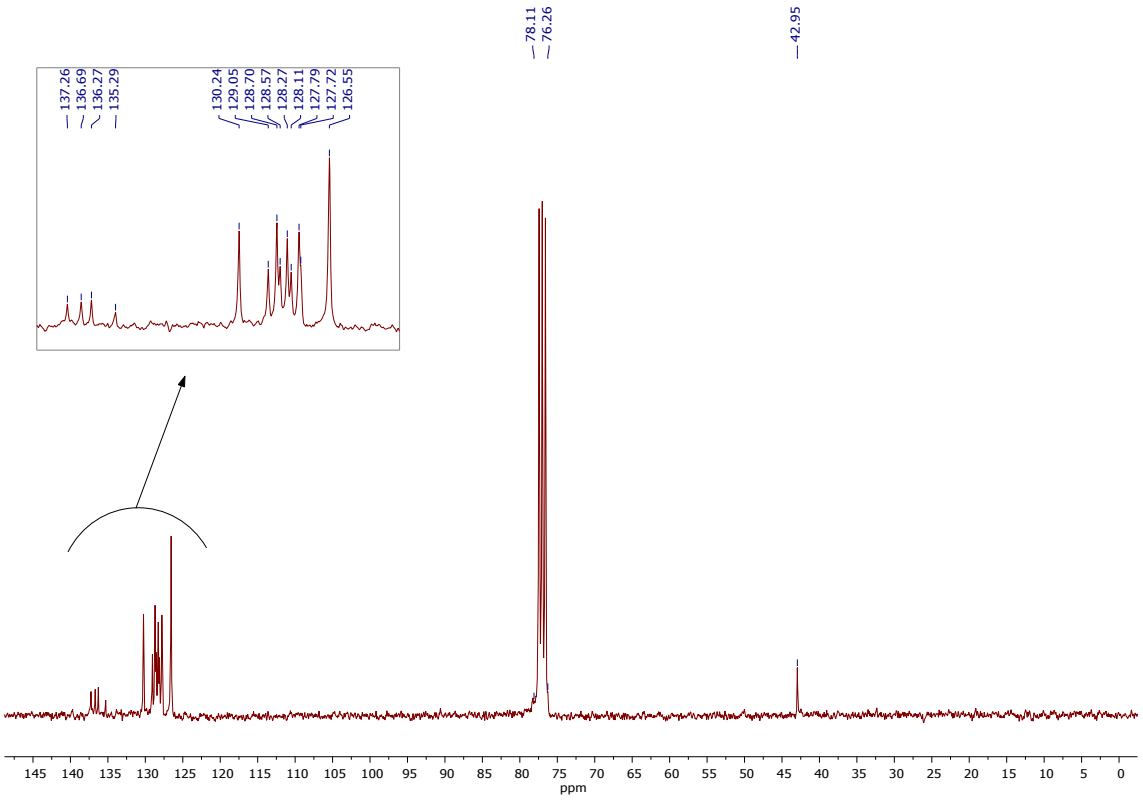

Compound **13**

^{1}H NMR ($CDCl_3$, TMS)

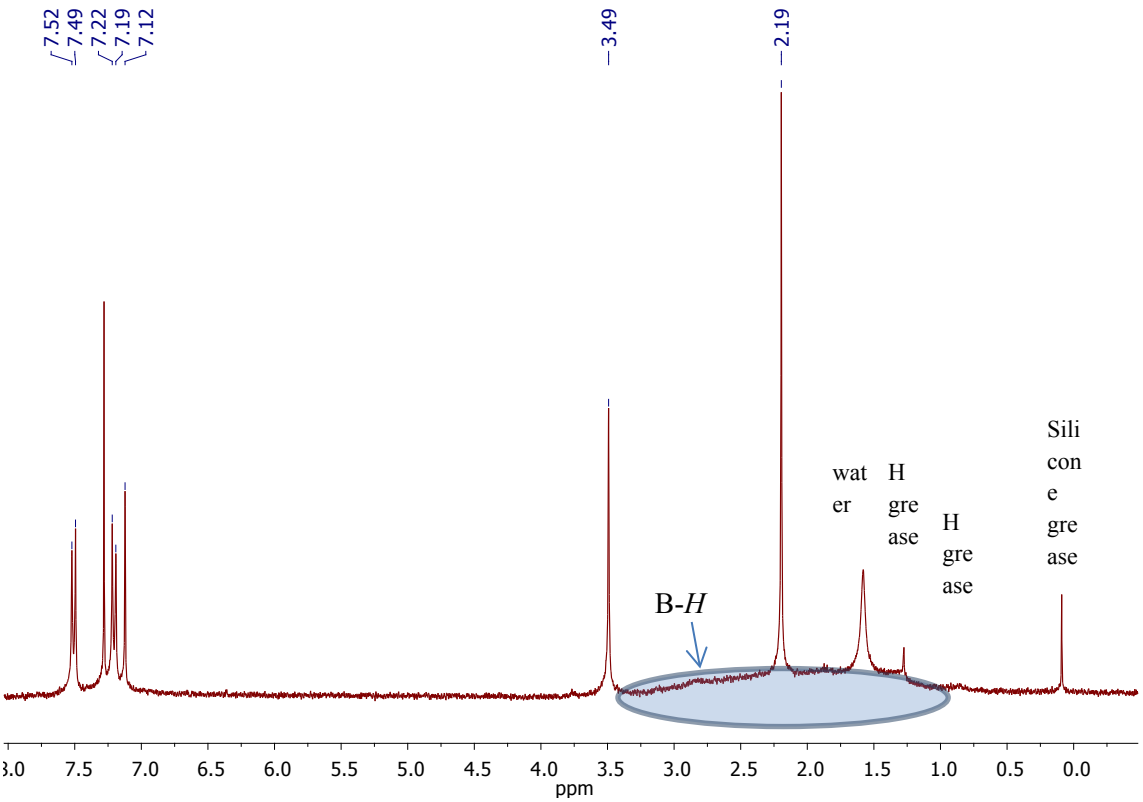

$^{1}H\{^{11}B\}$ NMR ($CDCl_3$, TMS)

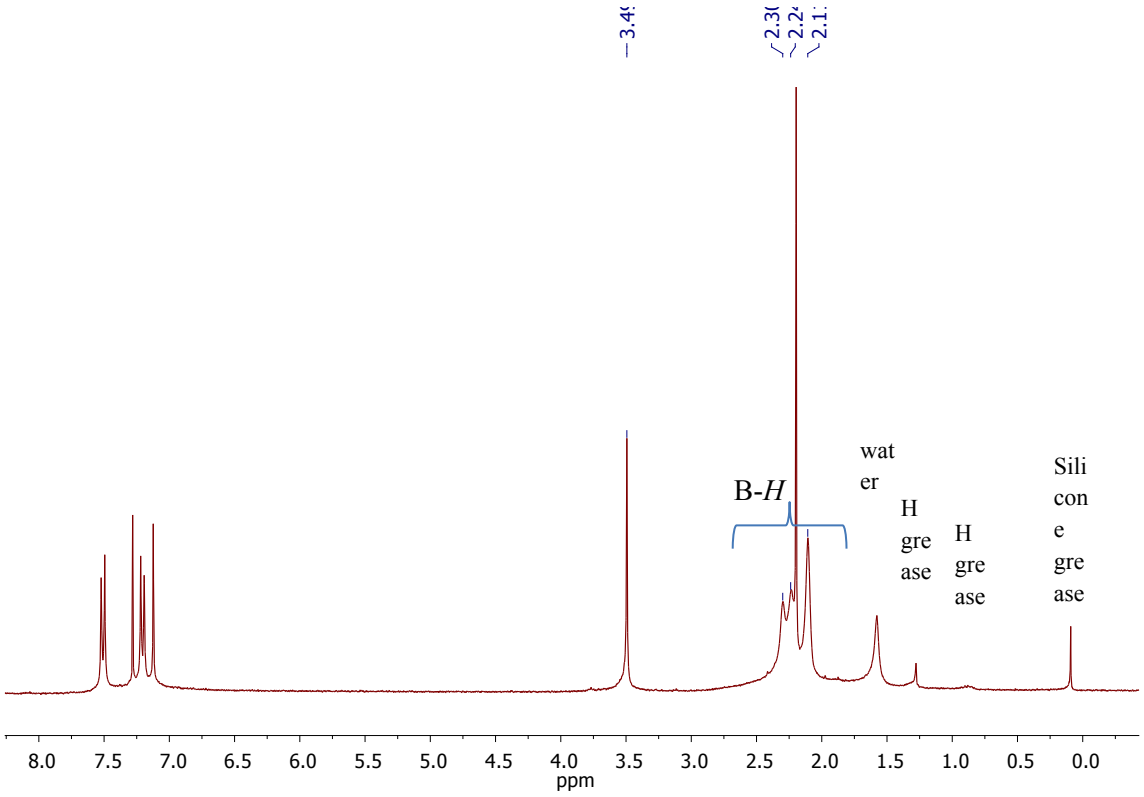

$^{11}B\{^{1}H\}$ NMR ($CDCl_3$, $BF_3{\cdot}Et_2O$)

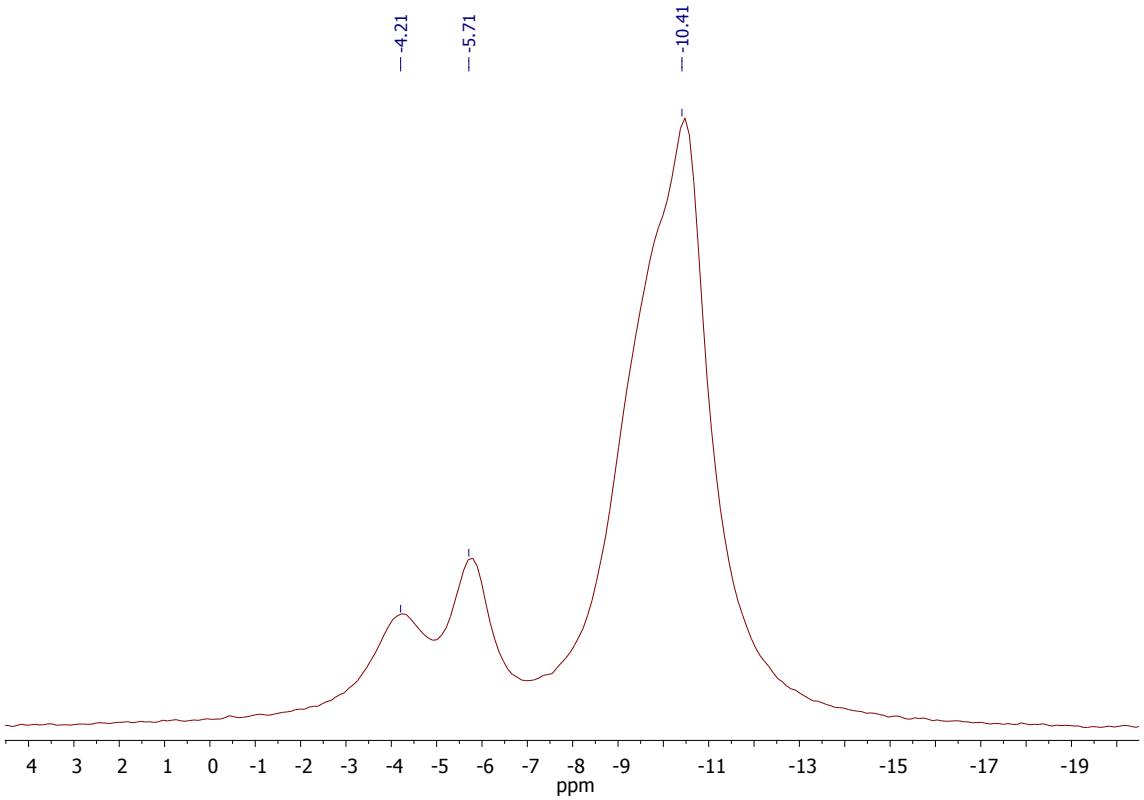

$^{13}C\{^{1}H\}$ NMR ($CDCl_3$, TMS)

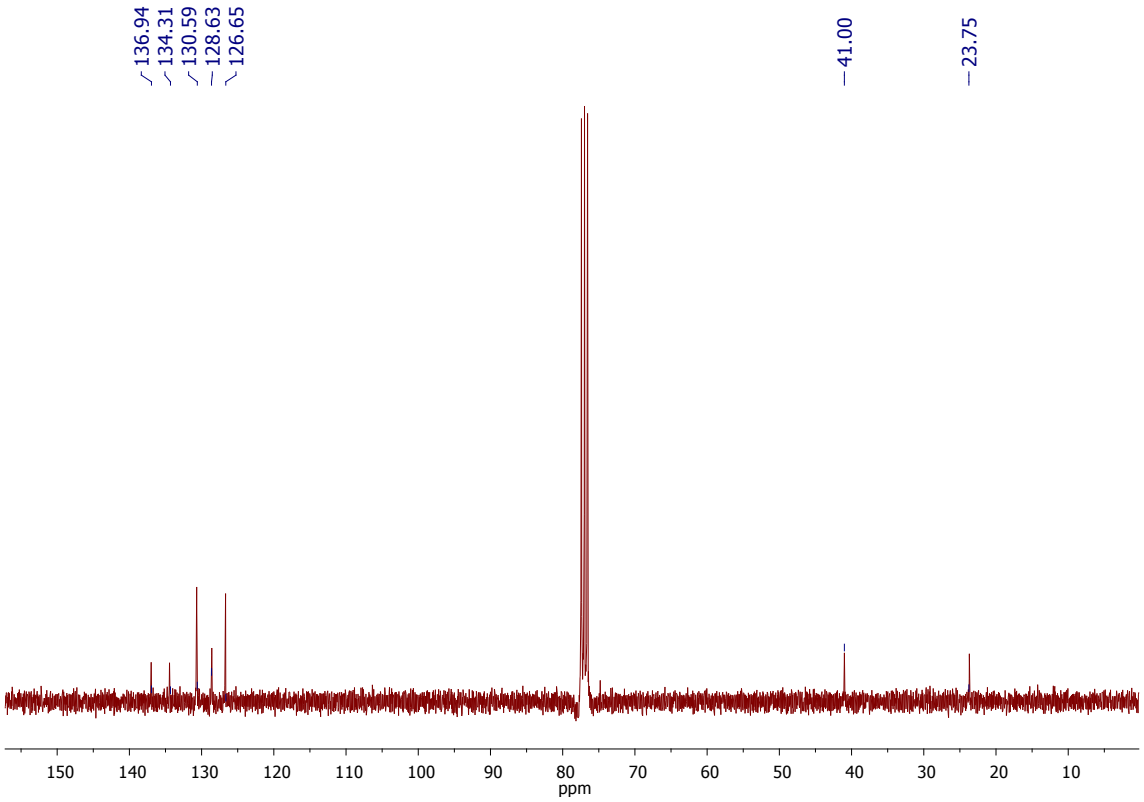

Compound **14**

^{1}H NMR ($CDCl_3$, TMS)

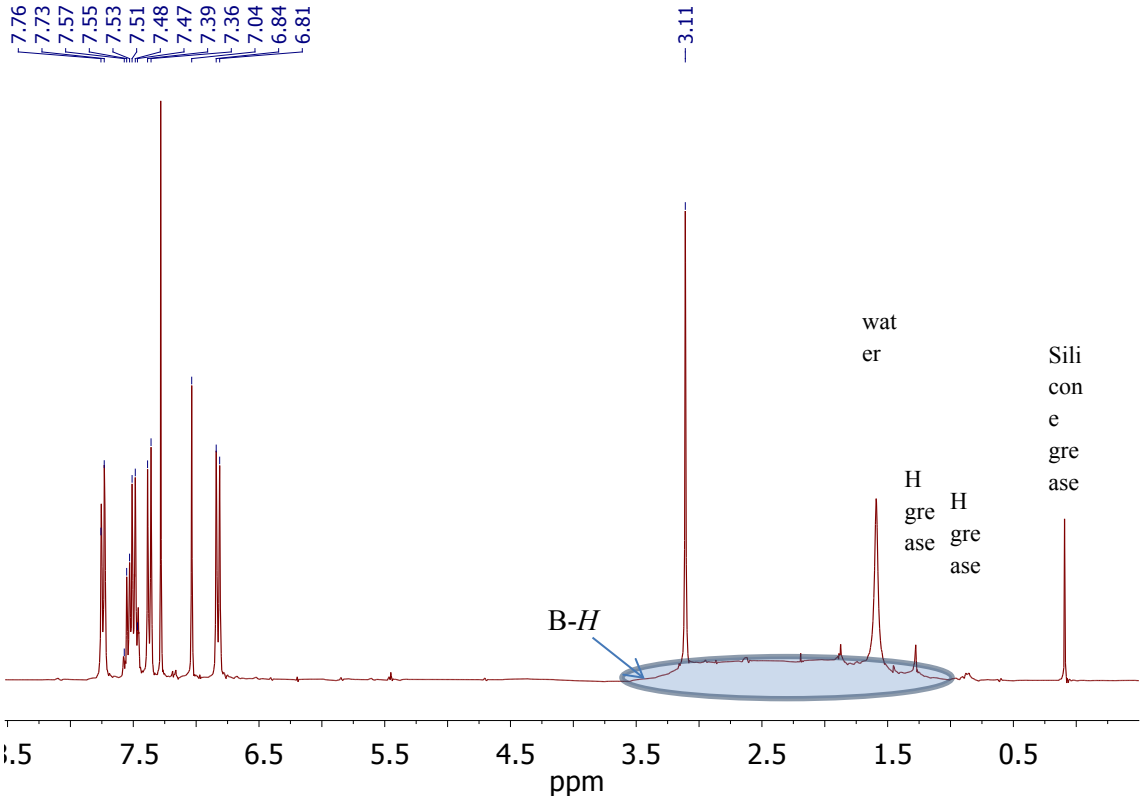

$^{1}H\{^{11}B\}$ NMR ($CDCl_3$, TMS)

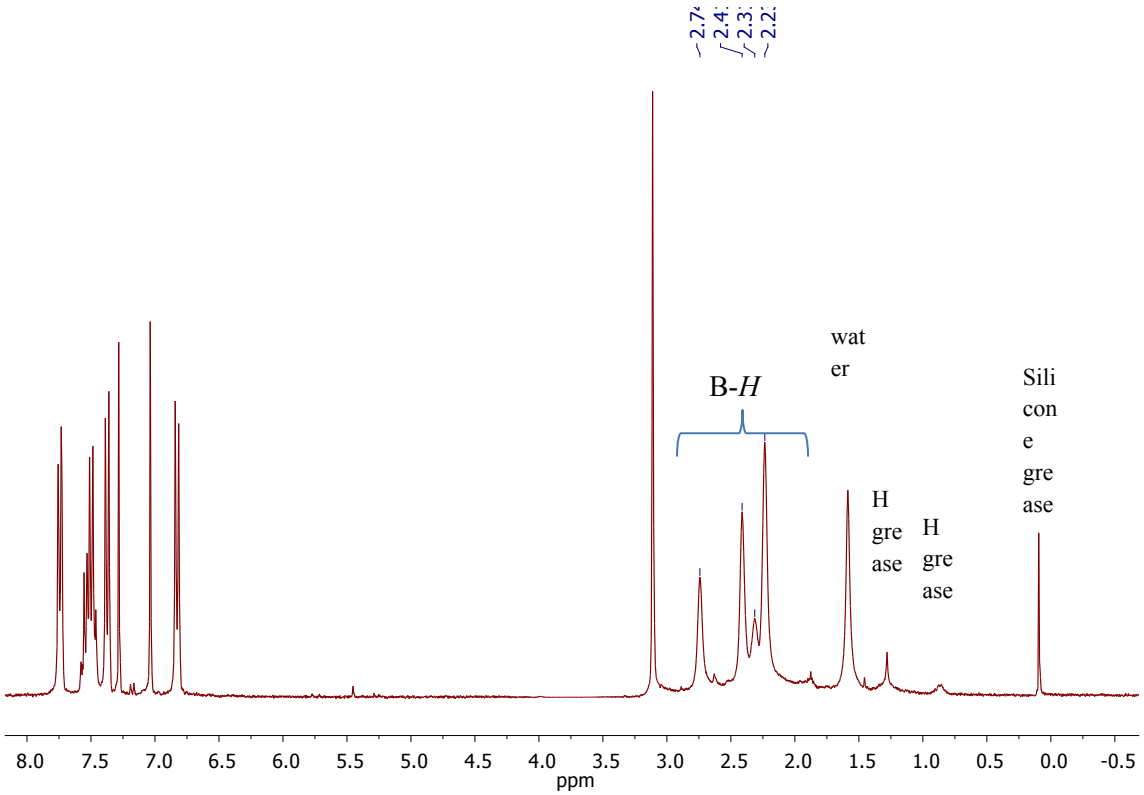

$^{11}B\{^{1}H\}$ NMR ($CDCl_3$, $BF_3{\cdot}Et_2O$)

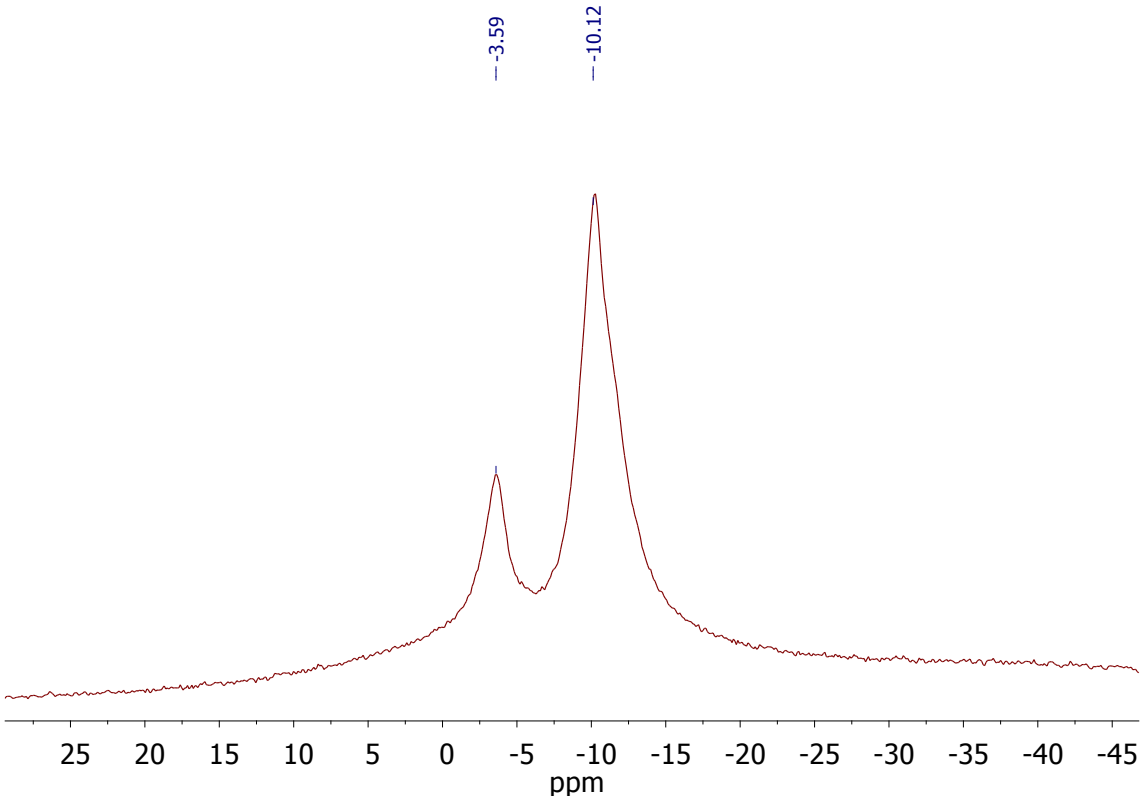

$^{13}C\{^{1}H\}$ NMR ($CDCl_3$, TMS)

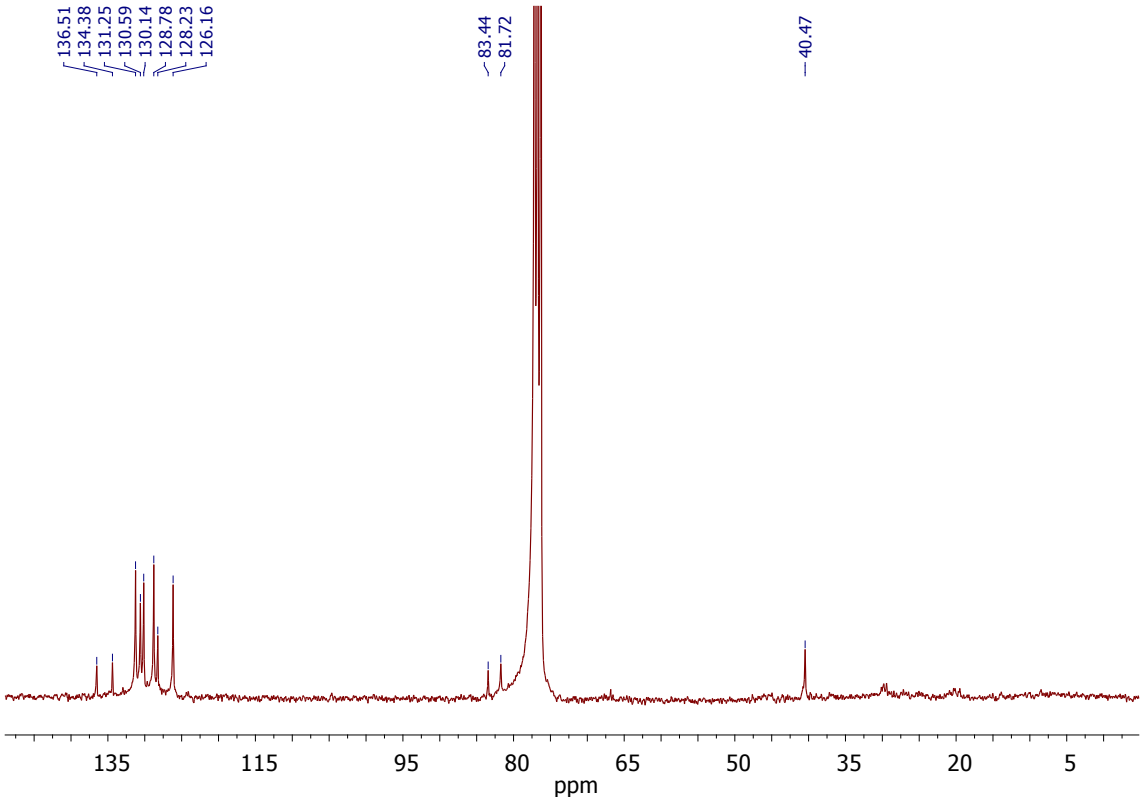

Compound **15**

^{1}H NMR ($CDCl_3$, TMS)

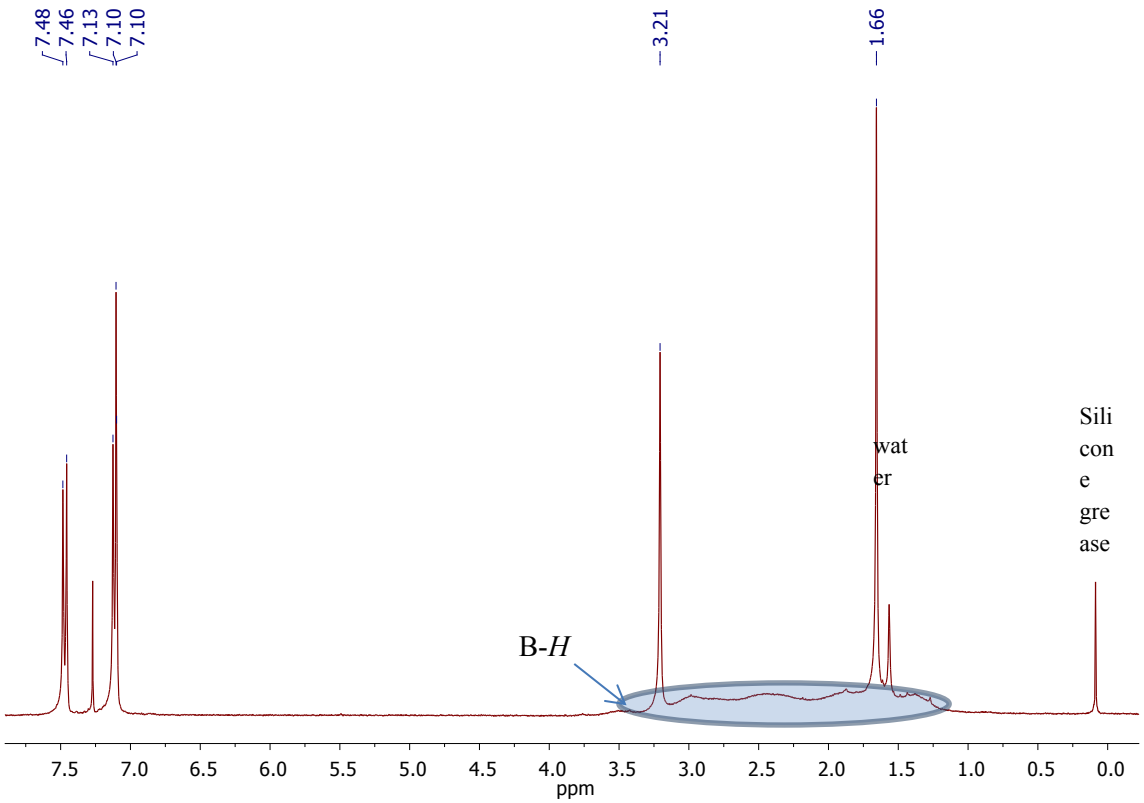

$^{1}H\{^{11}B\}$ NMR ($CDCl_3$, TMS)

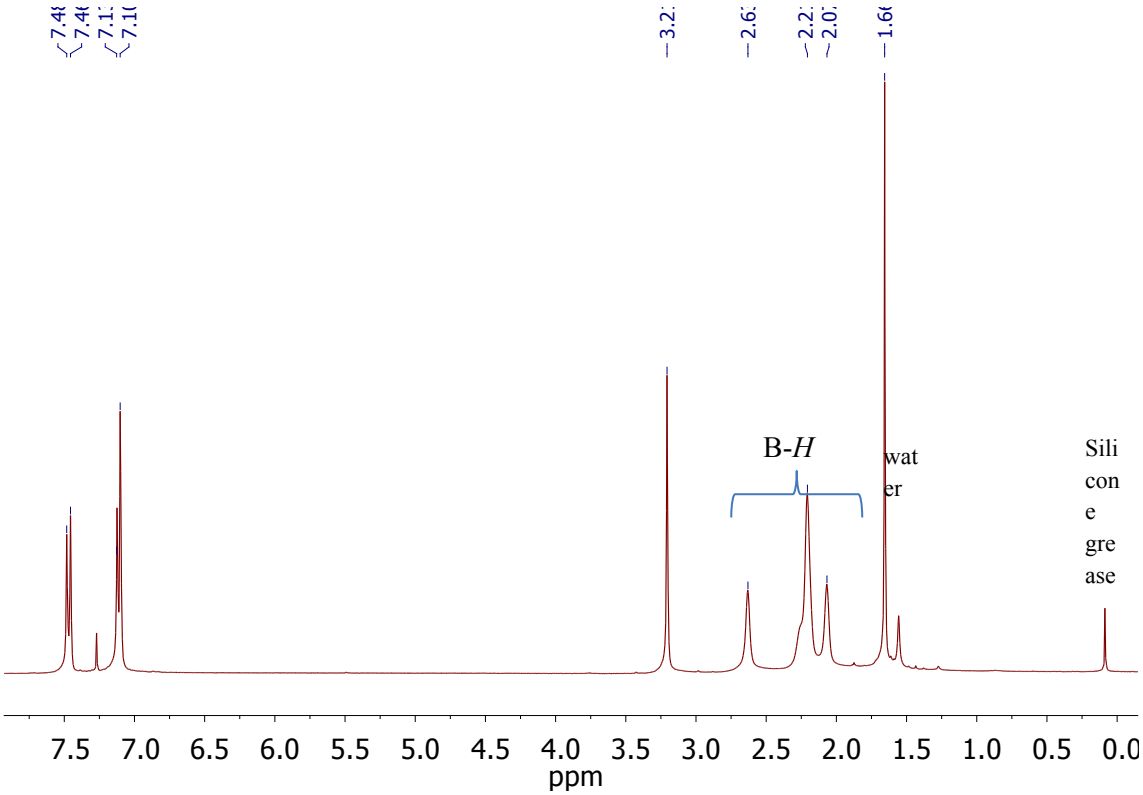

$^{11}B\{^{1}H\}$ NMR ($CDCl_3$, $BF_3{\cdot}Et_2O$)

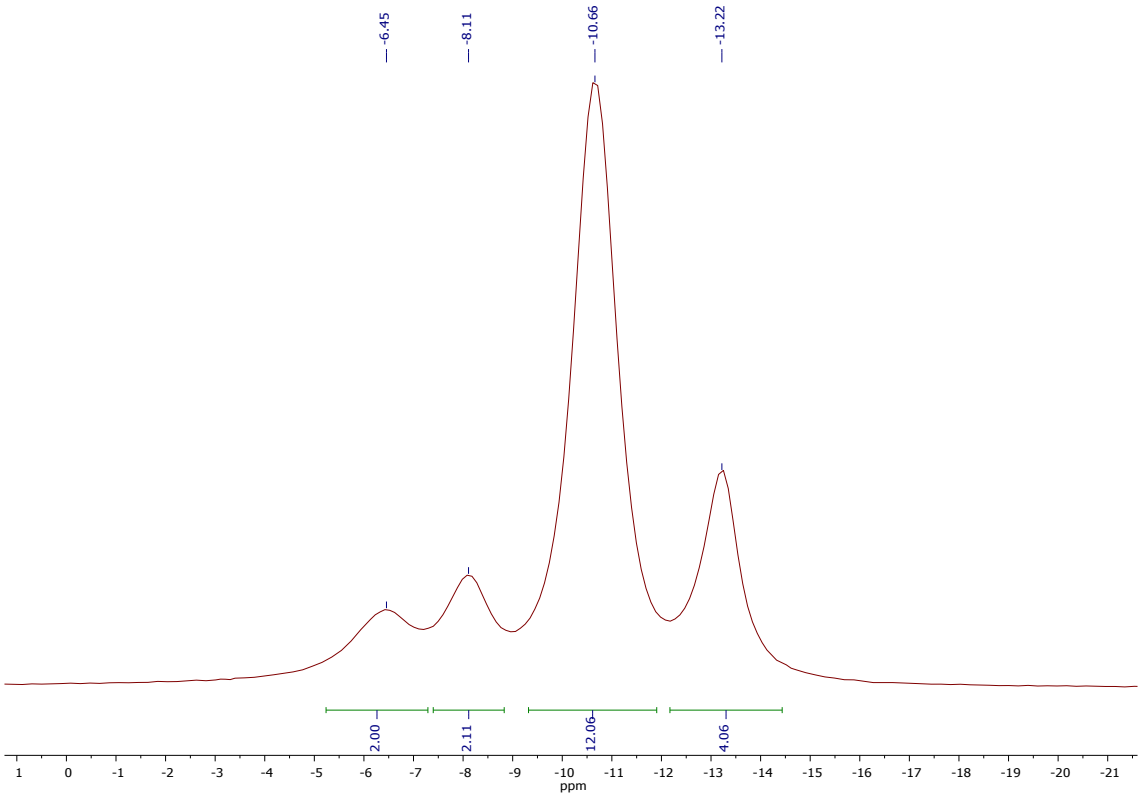

$^{13}C\{^{1}H\}$ NMR ($CDCl_3$, TMS)

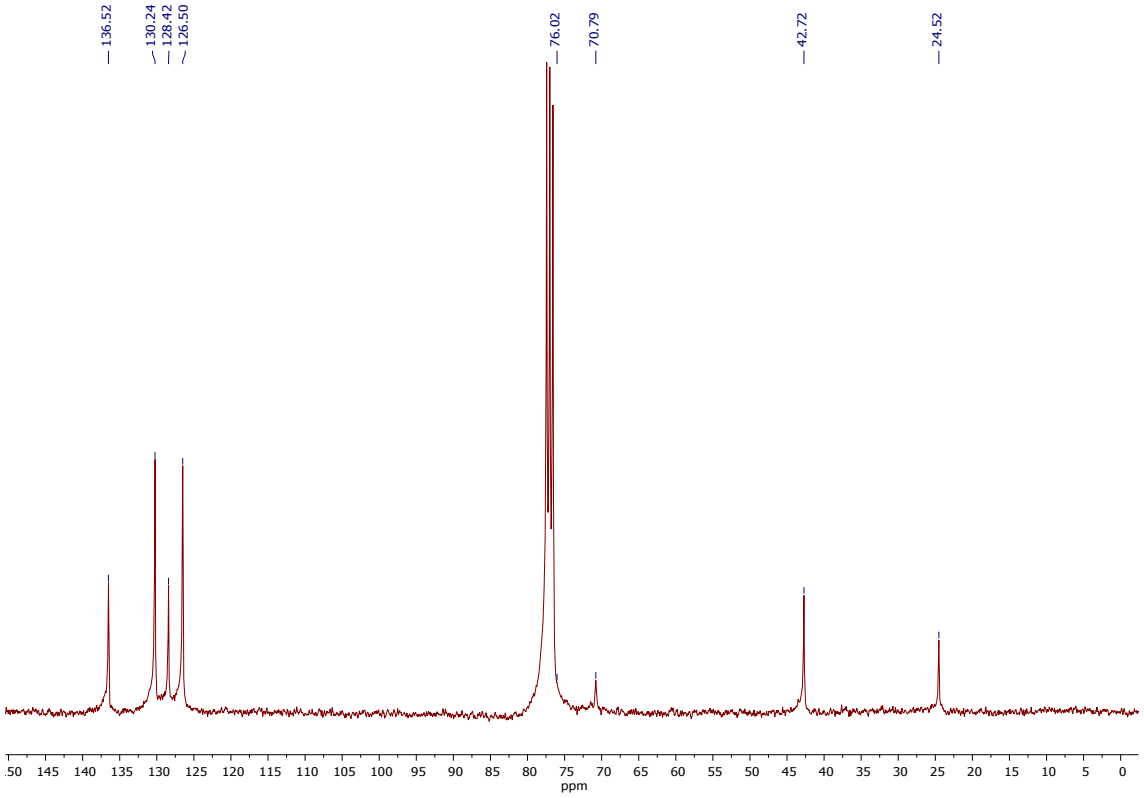

Compound **16**

^{1}H NMR ($CDCl_3$, TMS)

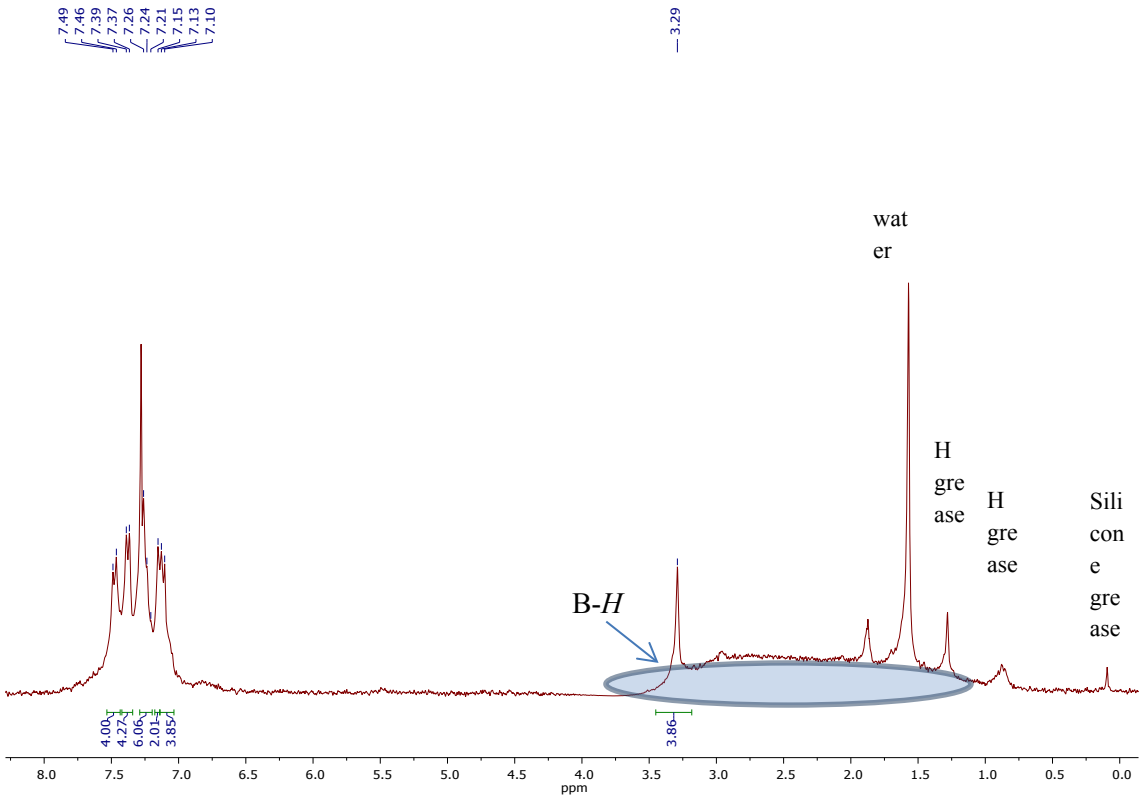

$^{1}H\{^{11}B\}$ NMR ($CDCl_3$, TMS)

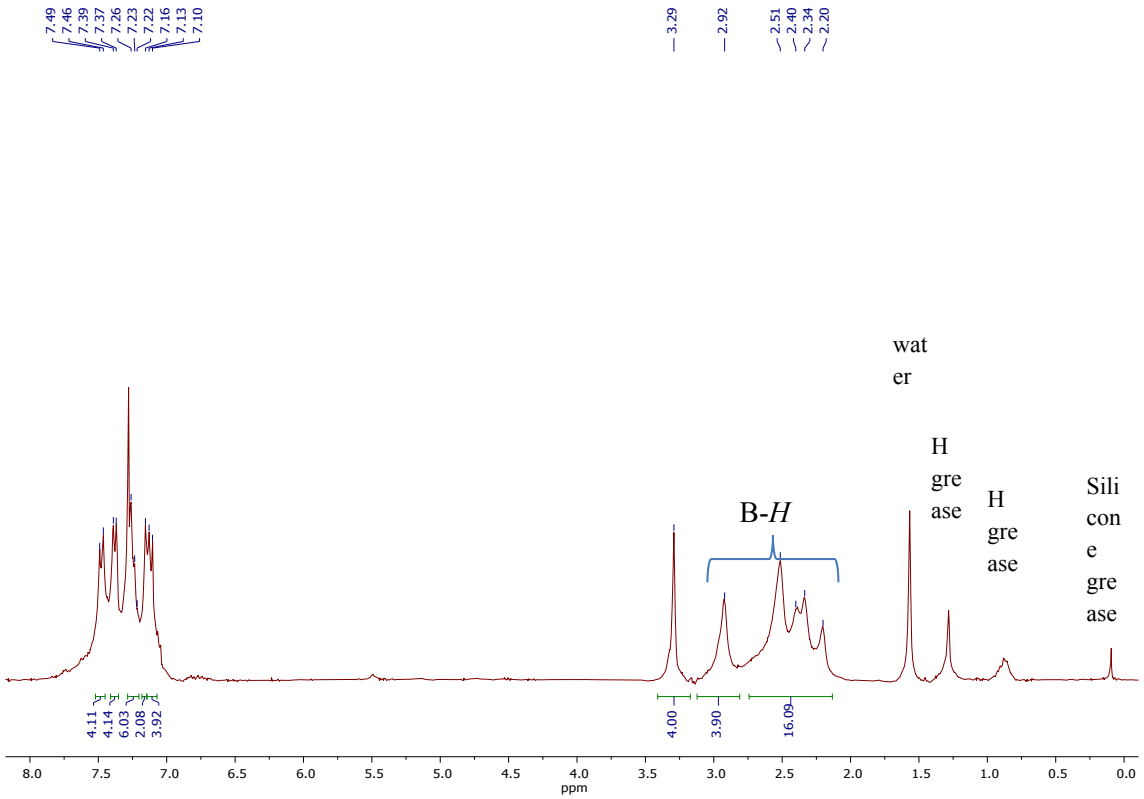

$^{11}B\{^{1}H\}$ NMR ($CDCl_3$, $BF_3{\cdot}Et_2O$)

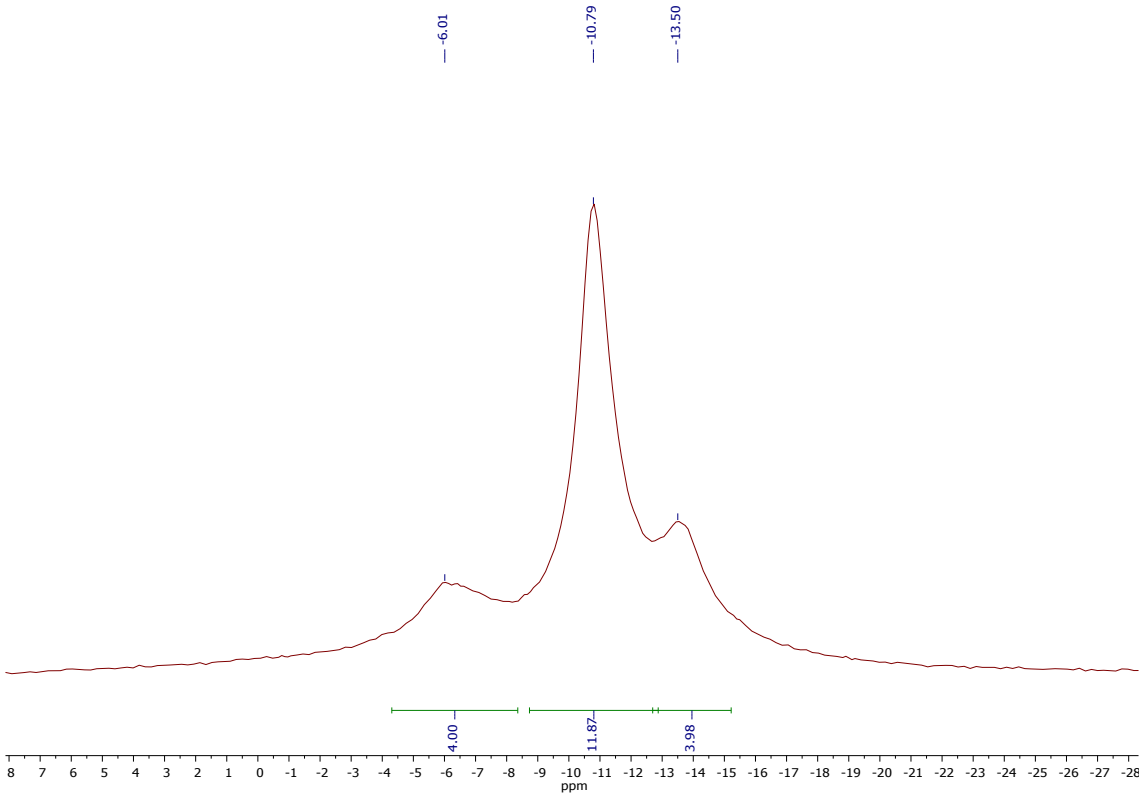

$^{13}C\{^{1}H\}$ NMR ($CDCl_3$, TMS)

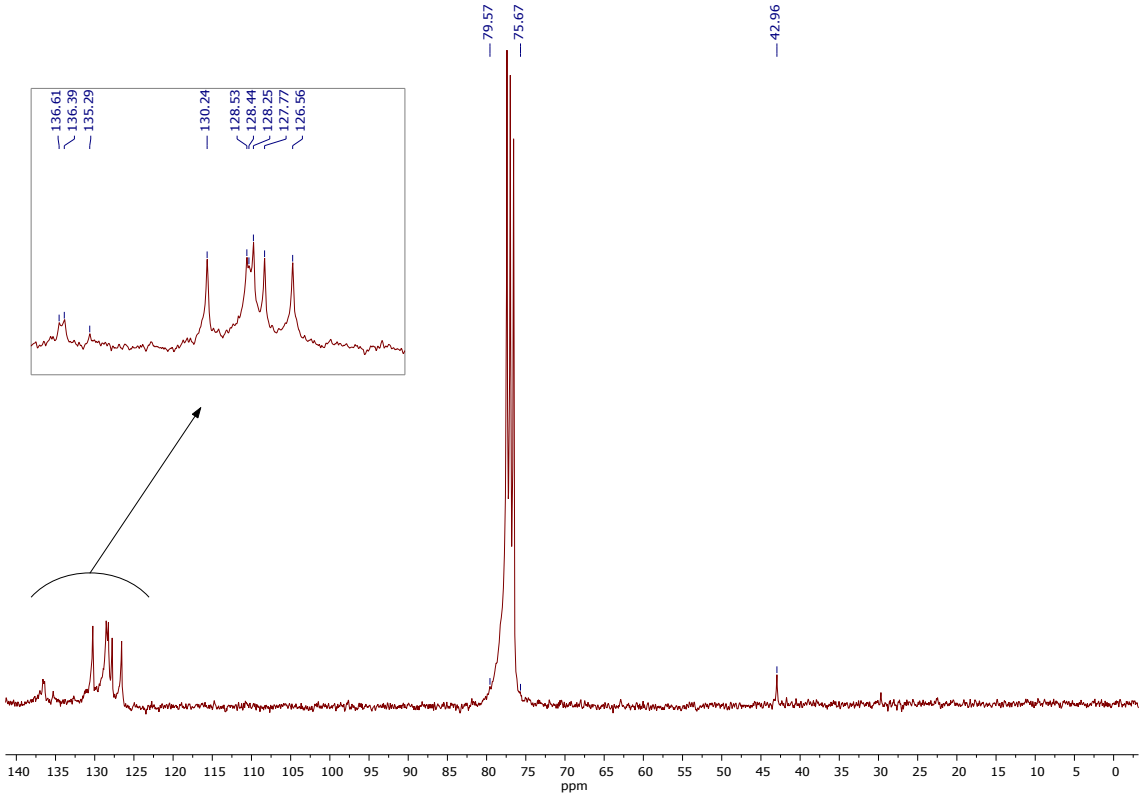

References

1 S. Dhami, A. J. D. Mello, G. Rumbles, S. M. Bishop, D. Phillips and A. Beeby, *Photochem. Photobiol.*, 1995, **61**, 341-346.
2 A. M. Brouwer, *Pure Appl. Chem.*, 2011, **83**, 2213-2228.
3 Y. Hong, J. W. Y. Lam and B. Z. Tang, *Chem. Soc. Rev.*, 2011, **40**, 5361-5388.
4 M. Tominaga, H. Naito, Y. Morisaki and Y. Chujo, *New J. Chem.*, 2014, **38**, 5686-5690.
5 K. Kokado and Y. Chujo, *J. Org. Chem.*, 2011, **76**, 316-319.
6 Z. Otwinowski and W. Minor, *Methods Enzymol.*, 1997, **276**, 307-326.
7 CrysAlisPro, *Journal*, 2015.
8 G. M. Sheldrick, *Acta Crystallogr., Sect. A*, 2008, **64**, 112-122.
9 L. Palatinus and G. Chapuis, *J. Appl. Crystallogr.*, 2007, **40**, 786-790.
10 G. Sheldrick, *Journal*, 2012.
11 F. Weigend and R. Ahlrichs, *Phys. Chem. Chem. Phys.*, 2005, **7**, 3297-3305.
12 A. Schäfer, H. Horn and R. Ahlrichs, *J. Chem. Phys.*, 1992, **97**, 2571-2577.
13 F. Neese, *Wiley Interdiscip. Rev.: Comput. Mol. Sci.*, 2012, **2**, 73-78.
14 T. Lu and F. Chen, *J. Comput. Chem.*, 2012, **33**, 580-592.
15 L. Tian and C. Feiwu, *Acta Chim. Sinica*, 2011, **69**, 2393-2406.
16 A.-R. Allouche, *J. Comput. Chem.*, 2011, **32**, 174-182.
17 A. Ferrer-Ugalde, E. J. Juárez-Pérez, F. Teixidor, C. Viñas, R. Sillanpää, E. Pérez-Inestrosa and R. Núñez, *Chem. Eur. J.*, 2012, **18**, 544-553.
18 L. J. Todd and A. R. Siedle, *Prog. Nucl. Magn. Reson. Spectrosc.*, 1979, **13**, 87-176.